Univerza *v Ljubljani*
Fakulteta *za farmacijo*

EVA GERMOVŠEK

DIPLOMSKA NALOGA

UNIVERZITETNI ŠTUDIJ FARMACIJE

Ljubljana, 2012

UNIVERZA V LJUBLJANI

FAKULTETA ZA FARMACIJO

EVA GERMOVŠEK

DEFINING THE OPTIMAL INFUSION TIME FOR MEROPENEM IN NEONATES

OPTIMIZACIJA TRAJANJA INFUZIJE MEROPENEMA PRI NOVOROJENČKIH

Ljubljana, 2012

Diplomsko nalogo sem opravljala na UCL School of Pharmacy, London (eksperimentalni del) in na Fakulteti za farmacijo Univerze v Ljubljani pod mentorstvom izr. prof. dr. Iztoka Grabnarja in somentorstvom dr. Josepha F. Standinga.

ZAHVALA

Iskreno se zahvaljujem mentorju izr. prof. dr. Iztoku Grabnarju ter somentorju dr. Josephu F. Standingu za pomoč pri izdelavi diplomske naloge in za vse koristne nasvete. Zahvaljujem se tudi ostalim na UCL School of Pharmacy, ki so mi pomagali pri delu.

Prav tako se iskreno zahvaljujem svojim staršem, ki so mi študij omogočili, in ostalim članom družine za podporo. Hvala tudi prijateljicam in sošolkam za zaupanje, podporo in čas, ki smo ga preživele skupaj.

Izjava

Izjavljam, da sem diplomsko nalogo izdelala samostojno, pod mentorstvom izr. prof. dr. Iztoka Grabnarja in somentorstvom dr. Josepha F. Standinga.

Eva Germovšek

Ljubljana, april 2012

Predsednik diplomske komisije: prof. dr. Samo Kreft
Član diplomske komisije: asist. dr. Rok Frlan

CONTENTS

ABSTRACT

During early childhood the human body undergoes substantial changes. Its composition changes, i.e. compared to adults, infants have higher total body water content and lower levels of plasma proteins. Liver function is decreased in neonates and so is renal elimination of drugs. The differences in body size can be taken into account by allometric scaling and maturation can be explained with a sigmoid Hill model.

Meropenem is an injectable broad spectrum β-lactam antibiotic of the carbapenem family. It penetrates well into most body tissues and fluids. It is primarily eliminated unchanged by the kidneys. Meropenem exhibits time-dependent killing, thus percentage of dosing interval when its concentration is above minimal inhibitory concentration (MIC) has to be at least 40% for bactericidal effect, and 20% for bacteriostatic effect.

Data from 19 preterm neonates were included in this study. Nine of them were given infusion of meropenem over 30 minutes and 10 of them over 4 hours. During the 12-hour dosing interval 6 blood samples per subject were taken and time of the sampling, dose, infusion length, plasma concentration of meropenem, and demographic characteristics of the subjects were recorded. The data were analysed using the non-linear mixed effects modelling software NONMEM and a population pharmacokinetic model for meropenem was developed. The influence of growth and maturation of the neonates was taken into account with the use of allometric scaling (with exponent of 1 for volume of distribution and 0.632 for clearance) and maturation function where Hill coefficient and value of postmenstrual age at clearance maturation half-time followed values from a published study of human renal function maturation. For the optimization of the infusion time a utility function was used. Dose was fixed to a standard off-label dose for meropenem in neonates (20 mg/kg) and target set to 100% of time above MIC. One thousand simulated subjects were generated using demographics from a neonatal database and individual pharmacokinetic parameters from the pharmacokinetic model. Meropenem infusion time was firstly optimized for subjects with MIC distribution following the one from EUCAST database for *E. coli*. Secondly, we estimated optimal infusion time at susceptibility and resistance breakpoints for this microorganism.

Meropenem pharmacokinetics in neonates followed a 1-compartment model with proportional residual error model and between-subject variability modelled by exponential

model. Physiological parameterisation for clearance was used. Final estimate (relative standard error) for meropenem clearance was 7.95 L/h/70kg (6.81%) and 20.7 L/70kg (10.14%) for volume of distribution. For randomly assigned MIC values there was no single optimal infusion time. In datasets with different distribution of MIC values it varied from 1 to 10 h. The optimal infusion time was driven by influential individuals, who were assigned high MIC values. When MIC values were set for all subjects to susceptibility (2 mg/L) and resistance (8 mg/L) breakpoints for *E. coli*, the optimal infusion times were approximately 6 and 7 hours, respectively. Further investigation revealed that even shorter infusion lengths (bolus IV, 0.5, 1, 2, 4 hours) provided sufficient percentage of time above MIC for meropenem bacteriostatic and even bactericidal effect. These results show that for infections in neonates, caused by microorganisms with resistance breakpoint of 8 mg/L or lower, it is not expected that antimicrobial efficacy of meropenem would be influenced by infusion time.

POVZETEK

Uvod

Človeško telo se od otroštva do odrasle dobe zelo spremeni. Spremeni se sestava telesa, npr. novorojenčki in dojenčki imajo večji delež vode v telesu (80-90%) v primerjavi z odraslimi (55-60%). Prav tako je pri dojenčkih relativno manj plazemskih proteinov, kar privede do večjih deležev nevezanih učinkovin in posledično tudi do večjih volumnov porazdelitve kot pri odraslih. Metabolizem večine učinkovin je zmanjšan pri novorojenčkih, saj jetrna funkcija še ni do konca razvita. Večina jetrnih encimov doseže odraslo aktivnost v prvem letu starosti. Zaradi nižje hitrosti glomerulne filtracije je tudi eliminacija zdravilnih učinkovin preko ledvic pri dojenčkih zmanjšana.

Ker farmakokinetični procesi (absorpcija, distribucija, metabolizem, eliminacija) pri dojenčkih še niso popolnoma razviti, moramo zanje pripraviti poseben režim odmerjanja. Razlike v velikosti med otroki in odraslimi lahko opišemo z alometrično enačbo, ki opisuje razmerje med velikostjo telesa in fiziološko funkcijo nekega organa, npr. eliminacijo. Dozorevanje procesov v telesu, npr. hitrosti glomerulne filtracije, pa lahko opišemo s sigmoidno Hillovo funkcijo.

Meropenem je β-laktamski antibiotik iz družine karbapenemov. Ima zelo širok spekter protimikrobne aktivnosti in je učinkovit proti mnogim aerobnim in anaerobnim grampozitivnim in gramnegativnim mikroorganizmom. Pri peroralni aplikaciji ne pride do absorpcije, zato ga moramo dati intravensko. Dobro se porazdeljuje v večino telesnih tkiv in tekočin in se v veliki meri (75%) izloča nespremenjen preko ledvic. Učinkovitost zdravljenja z meropenemom je odvisna od deleža odmernega intervala, ko je njegova plazemska koncentracija nad minimalno inhibitorno koncentracijo (MIC). Za baktericidno delovanje mora biti ta delež vsaj 40% in za bakteriostatičen učinek vsaj 20%. Zdravljenje z meropenemom pri novorojenčkih regulatorno ni odobreno, a se kljub temu pogosto uporablja nenamensko (angl. *off-label*).

Metode

V naši raziskavi smo zajeli 19 nedonošenih novorojenčkov (7 punčk in 12 fantkov) z zelo nizko porodno težo. Na oddelku za neonatalno intenzivno nego bolnišnic v Tartuju in Talinu (Estonija) so bili z meropenemom zdravljeni v večini primerov zaradi sepse. Devet

novorojenčkov je vsakih 12 ur dobivalo pol-urno in deset štiri-urno infuzijo antibiotika v odmerku 20 mg/kg. Vsakemu dojenčku so vzeli 6 vzorcev krvi: takoj pred infuzijo in potem pol ure, uro in pol, 4, 8 in 12 ur po začetku infuzije. Določili in zabeležili so čas odvzema vzorca, odmerek meropenema, dolžino trajanja infuzije, plazemsko koncentracijo meropenema in demografske podatke pacientov.

Na osnovi pridobljenih podatkov smo z uporabo programskega paketa za nelinearno modeliranje mešanih učinkov NONMEM razvili populacijski farmakokinetični model. Vpliv velikosti in dozorevanja novorojenčkov in njihove ledvične funkcije smo opisali z uporabo alometrične in Hillove enačbe. Pri alometrični enačbi je bil alometrični eksponent za volumen porazdelitve 1, v primeru očistka pa 0,632. Pri Hillovi sigmoidni enačbi je bil Hillov koeficient nastavljen na 3,33 in vrednost pomenstrualne starosti dojenčka, pri kateri ima očistek polovico vrednosti odraslega, na 55,4 tedne. Te vrednosti smo vzeli iz objavljene raziskave o dozorevanju ledvične funkcije.

Pri optimizaciji trajanja infuzije pri novorojenčkih smo uporabili funkcijo uporabnosti (angl. *utility function*). Tak način optimizacije je hitrejši in enostavnejši od sistematičnega spreminjanja trajanja infuzije za vse možne režime odmerjanja in ocenjevanja primernosti posameznega režima s populacijskim farmakokinetičnim modelom. Odmerek meropenema smo pri optimizaciji nastavili na 20 mg/kg, kar je običajno uporabljen odmerek za novorojenčke, cilj pa na 100% časa nad MIC. Z uporabo demografskih podatkov iz neonatalne zbirke in s pomočjo razvitega farmakokinetičnega modela smo simulirali tisoč pacientov. Le-tem smo nato z uporabo podatkov o porazdelitvi MIC (iz EUCAST zbirke za *E. coli*) določili individualno vrednost MIC, ki se je ujemala s porazdelitvijo iz EUCAST zbirke. Na osnovi tako pripravljenih podatkov smo določili optimalno trajanje infuzije meropenema. Proučevali pa smo tudi optimalno trajanje infuzije pri konstantni vrednosti MIC 2 mg/L (mejna vrednost za občutljivost pri *E. coli*) in 8 mg/L (mejna vrednost za odporne seve).

Rezultati

Končni populacijski farmakokinetični model za meropenem je bil enoprostorski model s proporcionalnim modelom rezidualne napake in logaritemsko porazdeljeno interindividualno variabilnostjo. Povprečna vrednost očistka meropenema je bila 7,95 L/h/70kg (z relativno standardno napako 6,81%), volumen porazdelitve pa je bil 20,7 L/70kg (10,14%).

Za naključno porazdeljene MIC vrednosti v simulirani populaciji 1000 pacientov smo ugotovili, da ni mogoče določiti le enega optimalnega časa infuzije. Le-ta je bil pri različnih, a še vedno naključno porazdeljenih MIC vrednostih, v razponu od ene do desetih ur. Na optimalno trajanje infuzije so vplivali izstopajoči posamezniki z veliko večjo MIC vrednostjo kot ostali (npr. pri večini je bila vrednost 0,016 mg/L, nekateri pacienti pa so imeli vrednost tudi 2 in celo do 16 mg/L). Po nastavitvi vrednosti MIC za vse paciente na 2 in 8 mg/L smo določili, da je optimalno trajanje infuzije 6 ur v prvem in 7 ur v drugem primeru. Z nadaljnjim raziskovanjem smo ugotovili, da je tudi v primeru krajših infuzij (bolus injekcija, pol urna, 1-, 2- in 4-urna infuzija) delež časa nad MIC pri več kot 99.4% pacientov večji od 40%.

Sklep

Ugotovili smo, da če so MIC vrednosti naključno porazdeljene (tako, da sledijo distribuciji iz EUCAST zbirke) med simulirane nedonošene novorojenčke je optimalno trajanje infuzije v razponu od 1 do 10 ur, odvisno od porazdelitve MIC vrednosti. Če je vrednost MIC nastavljena za vse dojenčke na 2 mg/L (kar je mejna vrednost za občutljivost pri *E. coli*), je optimalno trajanje 6 ur; v primeru 8 mg/L (odpornostna mejna vrednost) pa je približno 7 ur. Vendar pa je tudi pri krajših infuzijah (bolus, pol urne, 1-4 urne) delež odmernega intervala s koncentracijo meropenema nad MIC dovolj velik, da zadostuje za bakteriostatično in tudi baktericidno delovanje meropenema. Na osnovi tega lahko sklepamo, da za infekcije pri novorojenčkih, povzročene z mikroorganizmi z odpornostno mejno vrednostjo manjšo ali enako 8 mg/L, trajanje infuzije ne vpliva na protimikrobno učinkovitost meropenema.

LIST OF ABBREVIATIONS

AUC	area under the curve
AUCipred	area under the curve calculated from individual predicted concentrations
AUCobs	area under the curve calculated from observed/measured concentrations
AUCpred	area under the curve calculated from population predicted concentrations
BSV	between-subject or interindividual variability
c_{max}	maximal plasma concentration
CI	confidence interval
CL	clearance
CNS	central nervous system
CWRES	conditional weighted residuals
CYP	cytochrome P450
DHP-I	dehydropeptidaze-I
DV	dependent variable, in our study concentration
EUCAST	European Committee on Antimicrobial Susceptibility Testing
FOCE	first order conditional estimation
GA	gestational age
GFR	glomerular filtration rate
GOF	goodness-of-fit
GTS	global two-stage
ICH	International Conference on Harmonisation
IM	intramuscularly
iOFV	individual objective function value
IPRED	individual predictions
IT2S	iterative two-stage
IV	intravenously
MIC	minimal inhibitory concentration
MRSA	methicillin-resistant *Staphylococcus aureus*
NAD	naïve average data
NONMEM	non-linear mixed effects model software
NPD	naïve pooled data
OFV	objective function value
PBP	penicillin binding protein

pcVPC	prediction-corrected visual predictive check
PD	pharmacodynamic
PE	prediction error
PI	prediction interval
PK	pharmacokinetic
PMA	postmenstrual age
PNA	postnatal age
PPC	posterior predictive check
PPK	population pharmacokinetic
PRED	population predictions
PWR	allometric exponent
RBF	renal blood flow
RPE	relative prediction error
RSE	relative standard error
SD	standard deviation
SE	standard error
STS	standard two-stage
T>MIC	the cumulative percentage of a dosing interval that the drug concentration exceeds the MIC of the bacteria at steady state pharmacokinetic conditions
$t_{1/2}$	plasma elimination half-time
T_{50}	maturation half-time
TVCL	typical/mean value of clearance in the population
TVV	typical/mean value of volume of distribution in the population
UHPLC	Ultra High Pressure Liquid Chromatography
V	volume of distribution
VPC	visual predictive check
WSV	within-subject or intraindividual variability
WT	body weight
ε	residual within-subject error; the difference between observed and predicted concentration for an individual
η	between-subject variability; the difference between value of pharmacokinetic parameter for an individual and typical value in the population
θ	typical value of a pharmacokinetic parameter
σ^2	variance of within-subject variability
ω^2	variance of between-subject variability

LIST OF FIGURES

LIST OF TABLES

1. INTRODUCTION

1.1 THE DIFFERENCE IN PHARMACOKINETICS BETWEEN CHILDREN AND ADULTS

During the first years of life the human body undergoes dramatic changes, which include changes in body composition (for example, fat and body water content, concentrations of plasma proteins), and function of organs that are important in metabolism (e.g., the liver) and excretion (e.g., the kidney). These changes are usually nonlinear in the early childhood, thus pharmacologically speaking we cannot just consider children "miniature" adults. According to International Conference on Harmonisation (ICH) guideline E11 [1] children can be divided into five age classes: preterm newborn infants (infants with their gestational age (GA), i.e. time between the last menstrual period and birth, less than 37 weeks [2]), term newborn infants (0 to 27 days), infants and toddlers (28 days to 23 months), children (2 to 11 years) and adolescents (12 to 16/18 years).

1.1.1 Absorption

Drugs are most commonly administered to children by extravascular routes, usually orally. Therapeutic agents administered in such way undergo absorption and must overcome several barriers (e.g., chemical, biologic, physical) in order to be absorbed. In neonates and infants drug absorption is altered, compared to adults. An important factor that may affect the absorption from stomach is gastric pH. At birth it is practically neutral, around 6-8, decreasing to adult pH levels of around 1-3 within 24 h of birth. After that production of gastric acid gradually declines and gastric acidity returns to neutral pH by day 8. On a per kilogram basis, adult levels are achieved by the age of 2-3 years [3, 4]. As a result, acid-labile drugs (such as penicillin) may exhibit greater absorption and achieve higher serum concentrations in infants than in adults. In contrast, the absorption of weak acidic drugs (e.g., phenobarbital) may be reduced [4, 5]; or it might not even be affected, as it could continue in the small intestine [3].

In neonates and infants gastric emptying (the rate of removal of a drug from the stomach) is delayed and in neonates emptying times of 6 to 8 h have been reported [6]. This might result in delayed absorption of the drug. It is unclear when exactly the gastric emptying

time approaches adult levels [3].

Absorption of drugs by other extravascular routes can also be altered by developmental changes. During infancy percutaneous absorption may be enhanced because of thinner stratum corneum, decreased subcutaneous fat layer, and far greater skin-surface-to-body-weight ratio [5]. Relative to adults, cutaneous perfusion and hydration of the epidermis is greater in children as well and contributes to increased percutaneous absorption in infants and children [7].

On the other hand, the rate of intramuscular absorption of drugs in neonates may be reduced as a result of reduced skeletal-muscle blood flow, decreased muscle mass and tone, and decreased muscle activity. But the blood flow varies considerably, so it might be even less predictable in children than in adults [3, 5].

Rectal absorption is thought not to be affected by maturation, but is expected to vary between different age groups of children [3].

1.1.2 Distribution

Drug distribution is influenced by several factors, which explain the differences between paediatric population and adults. These factors are: membrane permeability, protein-binding of drugs, tissue binding, and also extracellular fluid volume as a proportion of total body water. The apparent volume of distribution (V), which indicates the extent of drug distribution into body fluids and tissues and relates the amount of drug in the body to measured plasma concentration, provides a useful marker in assessing age-related changes in drug distribution [8]. The larger V a drug has, the higher dose of it is needed to achieve a target drug concentration.

Membrane permeability is especially high in preterm neonates, which increases the penetration of drugs into central nervous system (CNS) and may result in a toxic effect. Even in term newborns blood-brain barrier is not fully mature, but matures with increasing age, which decreases the penetration of drugs into CNS [3].

Total plasma protein levels are lower in the newborn relative to the adult. Furthermore, these proteins are qualitatively different and generally exhibit lower binding capacities in neonates. The plasma concentration of albumin is at birth approximately 20% lower than in adult and reaches adult values through the first year of life. High unbound fractions may lead to significantly larger values of V and enhanced distribution into tissues [3, 4].

Volume of distribution may be significantly affected by changes in body composition,

which are correlated with both gestational and postnatal age. In very young infants the total body water is high (80-90% of the body weight) while fat content is low (10-15% of the body weight). By adulthood the amount of total body water decreases to 55-60%. The extracellular water content decreases as well; in neonates it is about 45% of the body weight and then declines to only around 20% of the body weight in adulthood. As a result of these changes, water-soluble drugs (e.g., gentamicin, linezolid) have relatively higher volume of distribution in childhood than in adulthood. For lipophilic drugs (e.g., diazepam), which associate primarily with tissue, the influence of age on V is not that big, but their V is still smaller in neonates and very young infants comparing to adults [3-5, 9].

1.1.3 Metabolism

During the process of drug metabolism an endogenous or exogenous molecule undergoes a biotransformation by one or more enzymes, which results in a more hydrophilic moiety that is then easily excreted. Primarily metabolism takes place in the liver, but it can also occur to a lesser extent in the kidney, gastrointestinal tract, lung and blood [5]. Hepatic metabolism is conventionally divided into two phases. Phase I reactions include oxidation (mostly by cytochrome P450 (CYP)), reduction, and hydroxylation, which result in formation of more polar, water soluble molecules. Phase II reactions, which include conjugation, glucuronidation, sulphation, and acetylation, combine the therapeutic agent with small molecules (for example, glucuronide, sulphate, glycine). Both phase I and II reactions mature over time, phase I reactions are generally 50% of activity at birth and mature by the 1st year of life, while phase II reactions vary in activity at birth from 20 to 70% and mature at a slower rate; glucuronidation activity, for example, matures by 3-4 years of age [5, 8, 10].

Via four major isoenzyme pathways approximately 90-95% of all drugs are metabolised: CYP3A4, CYP2D6, CYP2C, and CYP1A2 [5, 8]. Individual CYP enzymes mature at a different rate. CYP3A4 izoenzyme pathway is responsible for metabolism of the greatest number of commonly used drugs. In utero it has a low activity, then rapidly develops within a week of life, and is expressed at 50% of adult values between the ages of 6 and 12 months of age. CPY2D6 affects approximately ¼ of drugs. Fetal livers express very low activity of this enzyme, which dramatically increases immediately postpartum, reaches approximately 30% of adult activity by the first month of life and completely matures by 1 year of age. Roughly 15% of drugs are metabolised by CYP2C pathway. Within the first

month of postnatal life it reaches 30-50% of eventual activity, and adult levels sometime after the first year of life. CYP1A2's pathway is responsible for the metabolism of only about 5% of drugs. In neonates CPY1A2 is low, and its activity reaches only ½ of adults by age 1 year. Adult activity levels are reached sometime after that time [4, 8].

Maturation patterns of phase II enzymes are quite unique for each enzyme as well. For example, fetal livers exhibit limited uridine 5'-diphospho-glucuronosyltransferase activity, which reaches ¼ of adult's activity by 3 months of age and adult levels by 6-30 months of age. In contrast, fetal, newborn and infant livers express significant sulfotransferase activity, making this a relatively sufficient pathway at birth [4].

1.1.4 Elimination

The most important routes of elimination of drugs are the bile and the kidneys; however, drugs can also be excreted through sweat, air, or other fluids. The major organ for elimination of drugs or their metabolites is the kidney, with renal excretion being the product of glomerular filtration, tubular secretion, and tubular reabsorption.

Human renal development involves two basic processes: morphologic formation, which occurs exclusively in utero, and the acquisition of function, which continues after birth to reach adult levels. Nephrogenesis, the formation of individual nephrons, occurs from the week 6-36 of gestation. After that, each kidney has approximately one million nephrons. It is not determined yet whether new nephrons can develop after birth in prematurely born infants. During gestation renal blood flow (RBF) and glomerular filtration rate (GFR) progressively increase and achieve full-time levels by the 32nd to 35th weeks of GA. The values observed in adults are bigger than dose at term, even when corrected for body weight, kidney weight, or body surface area [11]. After birth renal and intrarenal blood flow increases, resulting in a rise in GFR. In term neonates GFR is approximately 2-4 mL/min/1.73m^2, however in preterm neonates it can be much lower, even as low as 0.6 to 0.8 mL/min/1.73m^2. Within the first two weeks of life GFR increases dramatically and then gradually rises until it approaches adult levels at 8 to 12 months of age [7]. Renal functional maturation and postnatal improvements in GFR are correlated better with postmenstrual age (PMA), rather than postnatal age (PNA) [4]. PMA is GA plus PNA (time elapsed after birth, i.e. chronological age) [12]. In premature infants GFR values are lower and they exhibit a slower pattern of GFR development during the first two weeks of life, compared to a full-term infant. Once nephrogenesis and maturation of glomerular function

are completed, GFR in preterm infants should increase at the same rate as in full-term infants. However, some studies show that GFR still remained lower in 5-week old preterm neonates [4, 11]. Adult values for RBF, GFR, and kidney size for preterm infants may be achieved as late as by 8 years of life [11].

At birth, renal tubules are anatomically and functionally immature, however, by 1 year of age renal tubule maturation is completed and adult capacity is reached [4].

All in all, renal excretion in the newborn is reduced in spite of relatively rapid increase in GFR and tubular secretion rate [6]. For drugs, primarily eliminated by kidneys (such as antibiotics), treatment regimens should be individualized in an age-appropriate fashion.

1.2 SCALING FOR SIZE AND MATURATION

Pharmacokinetic (PK) processes, such as absorption, distribution, metabolism, and elimination are functionally immature in paediatric population and are the reason for unique differences in adult, infant and children PK parameters. Knowing that, we have to design specific dosage regimen for paediatric population. The difference in body size can be taken into account by the use of allometry and developmental maturation can be explained with a sigmoid hyperbolic model.

1.2.1 Allometric scaling

Allometry is a term that describes the nonlinear relationship between size and physiological function, for example drug elimination. This relationship is represented by Equation 1.1.

$$y = a \times WT^{PWR}$$
(Eq. 1.1)

where *y* is the biological characteristic to be predicted, *WT* is the body weight, and *a* and *PWR* are empirically derived constants, *a* being the allometric constant and *PWR* the allometric exponent [13-15].

Another version of this equation is Equation 1.2 [15], which might be easier to understand.

$$PK\ parameter_{paediatric} = PK\ parameter_{adult} \times \left(\frac{WT_{paediatric}}{WT_{adult}}\right)^{PWR} \qquad \text{(Eq. 1.2)}$$

where *PWR* is the allometric exponent and *WT* is body weight.

The value of allometric exponent (PWR) is not clearly defined. Most researchers [14] advocate the ¾ power law for metabolic rates, which has been theoretically explained using fractal geometry by West et al [16, 17]. However, there are some that question PWR being 0.75 [18, 19] and think that it should be ⅔ [20]. Hu et al suggest that both could be true; for drugs that are eliminated mainly by metabolism or combined metabolism and excretion, 0.75 could be used, and for substances that are excreted mainly by renal elimination 0.67 might be applied [21].

Typically, PWR assumes a value of 1 (when the PK parameter is directly proportional to age-dependent changes in body weight and thus changes linearly to body weight; for example drug volume of distribution), ¾ (when the PK parameter relates to age-related changes in physiological processes, e.g., drug clearance, GFR), or ⅔ (when the PK parameter is approximately proportional to age-dependent changes in body surface area) [13, 15]. For PK parameters, that are time-related, for example, heart or respiratory rate, drug half-times, the allometric exponent is ¼ [14].

In pharmacokinetic analyses the PWR is often fixed to the values mentioned before, especially if the uncertainty in the determination of the exponent is relatively large [21]. However, it can be estimated as well [14].

1.2.2   Maturation function

Infants do not just increase in size, the effect of which is accounted for by allometry, they also mature. Maturation cannot be described by allometric scaling. As a result, to predict clearance in paediatric population from adults, allometry alone does not suffice. We also need a maturation model or a function that accounts for the age-related increase in clearance [22].

The maturation function represents the fraction of adult typical function. It starts at zero and asymptotes to 1, i.e. the mature or adult value. PMA is used to describe the maturation of clearance. The maturation of clearance begins in utero, that is why PMA predicts the elimination of the drug better than PNA [13]. For the description of this maturation

process, the sigmoid hyperbolic or Hill model has been found useful (Equation 1.3) [23]:

$$MF = \frac{PMA^{Hill}}{T_{50}^{Hill} + PMA^{Hill}}$$ (Eq. 1.3)

where *MF* is maturation function, T_{50} represents the PMA at which maturation reaches half-time, and *Hill* coefficient is a sigmoidicity coefficient and relates to the slope of the maturation profile.

Glomerular filtration rate (GFR), which is used to describe renal function in adults and usually referenced to body surface area, is obtained by comparing the predicted GFR to the expected "normal" GFR. Unlike in adults, where the expected GFR is reasonably well known, the GFR in infants changes rapidly [24]. During childhood GFR matures with age and grows, i.e. increases in size [13]. These rapid changes make the definition of the expected "normal" GFR in neonates difficult, thus not defined well. To describe GFR a sigmoid hyperbolic function, which explains the gradual maturation of GFR at an early age, followed by a more rapid increase after birth, and then again slow rise until it reaches adult values, can be used [24]. Figure 1.1 illustrates the maturation of GFR, showing the predictions of a sigmoid hyperbolic function.

In a study by Rhodin et al [24] empirical estimate of PWR with a value of 0.632 was found. This PWR improved the fit on statistical grounds; however, it is not known whether it improved the predictions of GFR.

The predictions of creatinine production rate in premature neonates are not yet well established. That is why Anderson et al propose that dosing of drugs, cleared by the kidneys, should not be based on serum creatinine. Instead, the dosing should be based on GFR, predicted by using size and maturation only [13].
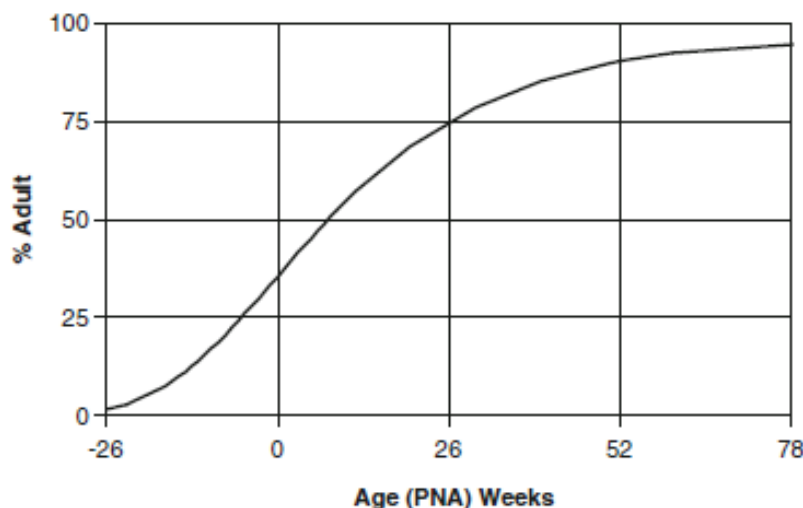
Figure 1.1: Maturation of glomerular filtration rate (GFR); on the x axis is postnatal age (PNA) in weeks, expressed so that at PNA=0 a full term infant with postmenstrual age of 40 weeks would be born; GFR follows the sigmoid hyperbolic function; from [24]

1.3 MEROPENEM

Pharmacokinetic (PK) and pharmacodynamic (PD) properties of meropenem define its efficacy. Serum concentration and the concentration in tissues reflect the absorption, distribution, metabolism and elimination of a drug; and the concentration of the drug in the body is what defines its PD properties.

1.3.1 Pharmacokinetic properties

In healthy adult subjects with normal renal function meropenem plasma elimination half-time ($t_{1/2}$) is approximately 1 hour [25-29]. In young infants and in preterm neonates the $t_{1/2}$ is longer, 2.9 [30] and 3.4 h [31], respectively. It is increased in patients with severe renal insufficiency as well, where it is approximately 5-fold higher than normal [32]. The steady-state volume of distribution in adults ranges from 12.5 to 23 L [25-27] or even to 33.6 L in Japanese adult population [33]. In preterm neonates V is around 0.74 L/kg [31] and 0.43 to 0.54 L/kg in young infants [30, 34], which is higher than in adults, when adjusted for weight. In patients, undergoing renal replacement therapy, meropenem V can increase to almost 70 L [35]. Meropenem clearance (CL) in adult population is between 11 and 18 L/h [25, 26, 36]. In preterm neonates mean CL is 0.157 L/h/kg [31] or 10.99 L/h/70kg, which

is almost the same as in adults. As expected, lower CL (3.4 L/h) is observed in patients with severe renal insufficiency [32].

Absorption

Meropenem is not orally absorbed, thus only available as a parenteral formulation. It can be administered either intravenously (IV) or intramuscularly (IM). When meropenem is given IM, its $t_{1/2}$ is slightly longer than in the IV route. Longer $t_{1/2}$ is probably related to slow absorption rate comparing to relatively rapid elimination. Peak plasma concentrations are at twice higher when meropenem is given as a 30-minute IV infusion comparing to the IM route of administration [25, 27].

Distribution

Meropenem exhibits predominantly extracellular distribution. It penetrates rapidly and substantially into most body tissues and fluids, including the cerebrospinal fluid, bile, muscle, skin, heart valves, pulmonary and gynaecological tissue, skin blister fluid and peritoneal fluid. Protein binding of meropenem is very low, only 2% [25, 27, 37].

Metabolism

Meropenem is a β-lactam antibiotic of the carbapenem family (Figure 1.2). The 1β-methyl substitution on the carbapenem ring makes meropenem relatively stable against renal dehydropeptidaze-I (DHP-I) compared to other carbapenems. Because of this reduced susceptibility there is no requirement to co-administer a DHP-I inhibitor, such as cilastatin. Meropenem undergoes both extrarenal and renal metabolism, which together account for approximately 25% of the total clearance. During the metabolism meropenem is subjected to hydrolysis, which produces its only metabolite, ICI 213,689. The metabolite is an open-ring β-lactam and is therefore bacteriologically inactive. About 75% of the administered dose is found unchanged in the urine [25, 27].
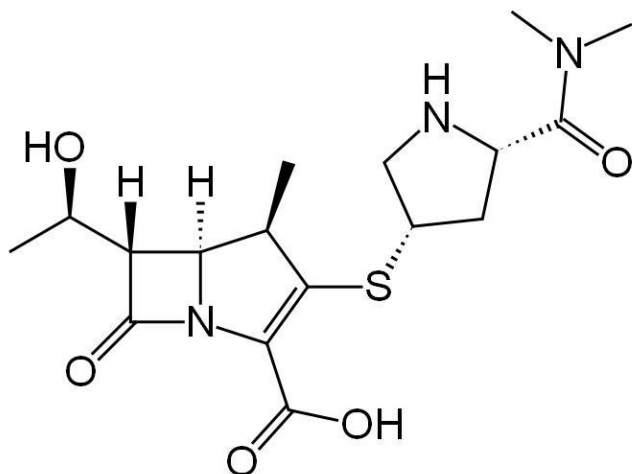
Figure 1.2: Chemical structure of β-lactam antibiotic meropenem

Elimination

Meropenem is primarily excreted unchanged by the kidneys within 12 hours. It has been established by probenicid interaction studies that meropenem undergoes both glomerular filtration and tubular secretion. Because of the predominant renal elimination, dosage adjustment for patients with severe renal impairment is required. On the other hand, the dose does not have to be adjusted for patients with hepatic insufficiency. The fecal elimination is negligible, only around 2% [25, 26, 38].

1.3.2   Pharmacodynamic properties

Mode of action

All β-lactam antibacterial agents bind covalently to penicillin binding proteins (PBPs), specific enzymatic proteins within the bacterial cell membrane. When a β-lactam binds to a specific PBP, it interrupts the transpeptidation (crosslinking) of peptidoglycan strands, a critical step in bacterial cell wall synthesis. This then results in bacterial cell death. Moreover, with binding to PBPs β-lactams can influence bacterial cells to activate the autolytic enzymes in the cell wall. These enzymes can cause lesions in the cell wall, which again leads to the death of the bacterial cell [26, 39, 40].

PK-PD relationship

There are two types of antibacterial activity. Antibiotics can exhibit time-dependent killing or concentration-dependent killing. In the first class are β-lactams (penicillins, cephalosporins, carbapenems, monobactams), macrolides (e.g., clarithromycin),

clindamycin and linezolid. To be effective, these antibiotics have to bind to microorganism for extensive amount of time. Aminoglycosides and fluoroquinolones are concentration-dependent drugs and eradicate the microorganisms with high concentrations at the binding site [39].

For time-dependent group of antibiotics it has been indicated that the percentage of a dosing interval that the drug concentration exceeds the minimal inhibitory concentration (MIC [41]) of the bacteria, i.e. time above MIC (T>MIC), is the best predictor of clinical outcome [39].

An antimicrobial drug can have bacteriostatic effect, i.e. it inhibits the growth of the microorganism, or bactericidal effect, meaning that it kills 99.99% of the bacterial population. The comparison of three β-lactam antibiotics (Table 1.1), specifically cephalosporins, penicillins and carbapenems, shows that for carbapenems the concentration of free drug must exceed the MIC for the smallest percentage of the dosing interval [42]. To obtain maximal bactericidal effect for carbapenem antibiotics T>MIC of free drug has to be at least 40% [37, 42, 43]. For bacteriostasis, the serum concentration of carbapenems has to be above MIC for only about 20% of the dosing interval [37, 42].

Table 1.1: Comparison of time above MIC between cephalosporins, penicillins, and carbapenems for bacteriostatic and bactericidal effects; adapted from [37, 42]

	Bacteriostatic effect (%)	Bactericidal effect (%)
Cephalosporins	35-40	60-70
Penicillins	30	50
Carbapenems	20	40

Spectrum of antimicrobial activity

Between β-lactams, carbapenem class is considered to be the most potent with the widest spectrum of antimicrobial activity. Carbapenems are effective against gram-positive and gram-negative aerobic and anaerobic microorganisms [44]. Meropenem, for example, is bactericidal against most strains of *Staphylococcus aureus*, *Enterococcus faecalis*, *Streptococcus pneumoniae* (penicillin-susceptible isolates only), *Escherichia coli*, *Haemophilus influenzae* (β-lactamase- and non-β-lactamase-producing), *Klebsiella pneumonia*, *Neisseria meningitidis*, *Pseudomonas aeruginosa*, and more. However, meropenem is not effective against methicillin-resistant *Staphylococcus aureus* (MRSA), vancomycin-resistant isolates of *Enterococcus faecalis*, *Staphylococcus epidermis*, and

amoxicillin-resistant *Enterococcus faecium* [38, 45]. Clinical MIC breakpoints from European Committee on Antimicrobial Susceptibility Testing (EUCAST) for some bacteria are shown in Table 1.2 [46].

Table 1.2: EUCAST clinical MIC breakpoints for meropenem (2012-01-01 version 2.0)

Organism	Susceptible (S) ≤ (mg/L)	Resistant (R) > (mg/L)
Enterobacteriaceae	2	8
Pseudomonas spp.	2	8
Acinetobacter spp.	2	8
Streptococcus pneumoniae[1]	2	2
Streptococcus pneumoniae (meningitis)	0.25	1
Other streptococci	2	2
Haemophilus influenzae[1]	2	2
Haemophilus influenzae (meningitis)	0.25	1
Gram-positive anaerobes[2]	2	8
Gram-negative anaerobes	2	8

[1]infections other than meningitis
[2]except *Clostridium difficile*
Adapted from [46]

Meropenem is indicated for the treatment of infections in children over 3 months of age and adults. These infections are: complicated skin and soft tissue infections, intra-abdominal infections (complicated appendicitis and peritonitis), and bacterial meningitis (only in paediatric patients, aged more than 3 months). Meropenem can also be used for the treatment of febrile neutropenia, bacterial meningitis (in adults), gynaecological infections, pneumonia, and complicated urinary tract infections [38, 45, 47].

1.4 POPULATION PHARMACOKINETIC MODELLING

The aim of population pharmacokinetic (PPK) modelling is to assess typical PK parameters of a drug and the variability on them. Furthermore, it can be used to provide guidelines for dosing regimens. The traditional approach to studying pharmacokinetics of a drug requires the subjects to be sampled intensively. But unfortunately this is not always possible, especially not in special populations, such as neonates, which have limited blood volumes. The PPK approach allows us to study sparse data as well and this is an important advantage [48].

Several methods can be applied to PPK modelling. These include naïve average and pooled data approach, the two stage approach, and nonlinear mixed-effects model approach.

1.4.1   Naïve average data approach

Analysis of the data from studies where all the subjects have been administered the drug at the same time can be done with naïve average data (NAD) approach. This is the case in experimental data studies with standardized designs, which include bioavailability and bioequivalence studies. The NAD approach is quite simple. The first step in this analysis is to average the data across individuals for each sampling time. This makes sense, since all the samples have been taken under identical conditions. The second step is to fit a model to the mean value and estimate the best-fit parameter values. Even just one fitting is enough to obtain estimates of parameters describing the mean response [49].

However, NAD approach has some disadvantages as well. Because of the smoothing effect of the data averaging, the peculiarities seen in the individual data can be clouded. The variability is masked, so there is no estimation on variability between subjects. Therefore, the NAD approach may be misleading and not the most reliable method for analysing the PPK data [49].

1.4.2   Naïve pooled data approach

The naïve pooled data (NPD) approach is far more general than the NAD approach. In NPD method all data from all individuals are considered to be from one unique reference subject. This approach fits all the data from subjects at once and obtains parameter estimates. The drawbacks of NPD approach are practically the same as in NAD approach. If the variations between subjects are small, which is unfortunately seldom the case for humans, the NPD approach can perform rather well. However, this approach is not really appropriate for data with imbalance and confounding correlations. Imbalance in the data can be caused by many more samples taken from one subject than the other, for example 5 and 1, respectively. This often occurs in the observational data and poses serious problems to NPD approach. As do the confounding correlations, meaning that the presence or absence of an observation is dependent on the subject's pharmacokinetics. Confounding correlations are frequently present in observational data, where they cannot always be prevented with randomization [49].

1.4.3   The two-stage approach

This approach comprises several methods. What is common to all of them is that there are two stages. In the first stage individual parameters are estimated by a separate fit of each subject's data. And in the second stage population parameter estimates are obtained by obtaining parameters across individuals [49].

Most commonly used and the simplest two-stage approach is the standard two-stage approach (STS). It is useful for pooling individual estimates of PK parameters from experimental PK studies. The results may not be the most valid, although it tends to overestimate parameter dispersion [49].

Other two-stage approach methods are global (GTS), iterative (IT2S), and Bayesian two-stage approach. The GTS provides unbiased estimates of the population mean parameters, while the estimates of the variances are biased. The IT2S is a method where the individual data is fitted repeatedly. This approach can be applied to rich and sparse data, as well as a mixture of both. The last one, the Bayesian two-stage approach, provides good estimates of population PK and PD parameters [49].

1.4.4   The nonlinear mixed-effects model approach

The nonlinear mixed-effects model can account for population PK parameter variability within or between subjects. This variability is predicted by random effects. It can also account for differences in parameter, which can be predicted by covariates (fixed effects) [50, 51].

Analysing the data

Typically the data used in this model is sparse. It usually ranges from 1 to 6 samples per subject. This modelling approach analyses the data of all individuals at once and at the same time takes random effects into account. Because of this it is appropriate for observational data with data imbalance and confounding correlations [49].

Computer program

The first modelling computer program for this approach was the non-linear mixed effects model software (NONMEM) [52]. NONMEM was originally developed by Stuart Beal, Lewis Sheiner, and Alison Boeckmann. In NONMEM software, the model is linearized by taking the first order Taylor series expansion with respect to the random effect variables

[49].

Variability

The PPK approaches allow us to estimate variability and also to identify its sources. Variability can be characterized with fixed effects (the population average values of PK parameters) and random effects, which quantify the amount of PK variability that is not explained by the fixed effects. There are two sources of random variability. One is the interindividual or between-subject variability (BSV) and the other is the intraindividual or within-subject variability (WSV) [48].

In NONMEM is the BSV modelled in terms of η variables. Each η is assumed to have a mean of 0 (because positive values cancel negative values) and a variance represented by ω^2. NONMEM software estimates initial estimates of ω^2 [50].

The residual or WSV is in NONMEM modelled in terms of ε variables. Residual variability is the difference between the model prediction for the individual subject and the observation. WSV includes the measuring error, errors in the assay, errors in drug dose, etc. ε is a normally distributed random variable with a mean of 0 and a variance of σ^2. Particular ε is random, so it is impossible to define it, but we can define its distribution [48, 50].

Evaluation

PKK models can be descriptive, i.e. they summarize PK variability in the studied population, and predictive, meaning they extrapolate beyond the population that was used to estimate the model. For descriptive models it is vital to assess their goodness of fit, reliability, and stability. Only this can assure efficient analysis of the data and generate reliable conclusions and predictions [53-55].

According to Brendel et al. [56], the evaluation methods can be divided into three categories by increasing order of quality. These categories are: basic internal methods, advanced internal methods and external methods for evaluation.

Basic internal methods include techniques, such as goodness-of-fit (GOF) plots, uncertainty on parameter estimates and model sensitivity to outliers. GOF plots are most commonly used in model evaluation and help to detect potential bias or problems in the

structural model and/or in the random effects model. GOF plots include several plots, e.g. observations (observed dependent variable, DV) versus population predictions (PRED) or individual population predictions (IPRED), conditional weighted residuals (CWRES) versus time or PRED. CWRES are calculated based on the first order conditional estimation (FOCE) approximation [57]. Most of these GOF plots are recommended by The European Medicines Agency as well [58]. Model reliability can be determined by evaluating the precision on parameter estimates from standard errors (SE) or confidence intervals (CI). Relative standard error (RSE) for mean and random effects parameters should not exceed 25% and 50%, respectively, in order to assure small uncertainty of model parameters [53, 56].

Advanced internal methods include data splitting, resampling techniques (such as bootstrapping and cross-validation), and Monte Carlo simulations, such as visual predictive check (VPC) or posterior predictive check (PPC). VPC is a commonly used and easily interpretable form of a PPC [59, 60]. It has many advantages, two of them being that the principle behind the diagnostic is simple and easily conversed to modellers and that by keeping the original time-course profile and the y-axis units, the VPC graphs are plotted on a scale which helps guiding modellers to the origin of a potential model misspecification [61]. VPC graphically assesses whether the model we are evaluating is able to reproduce the variability in observed data from which it originates. A typical VPC is based on multiple simulations made by using the model of interest and the design structure of the observed, original data (i.e. number of samples, dosing, and timing) [60, 62]. To make the interpretation of VPCs less subjective, we can look at the size of CI [61]. In ideal situation, VPC will diagnose both the fixed and the random effects in a mixed-effects model [63]. Traditional VPC has some limitations, for example it is inadequate for nonlinear PK models with different doses or with covariate effects [64]. A solution to these problems offers prediction-corrected VPC (pcVPC), while still keeping the visual interpretation of the traditional VPC [61].

External evaluation methods are based on comparison of the predictions obtained from the model (based on the learning dataset) to the new validation dataset [56].

In addition, metrics, such as prediction error (PE), and standardized prediction error can

also be used as techniques for model evaluation [56].

1.5 UTILITY FUNCTION

One could use PK-PD model to try to define the optimal dosing schedule, but since this would take individual evaluation of all possible dosing schedules, which would be very time consuming, this is not the best option. A better approach is to estimate an optimal dosing strategy by minimizing the risk function [65] or maximizing the utility function.

A utility function is a mathematical tool which helps us to assess the compromise between competing objectives [66]. For example, if we are trying to identify the optimal dose, the utility function would look at both, the efficacy and toxicity/intolerability. The utility function basically measures the usefulness of a particular estimation, e.g. optimal dose or optimal infusion length. In decision analysis this optimality criteria is commonly called utility function [67, 68].

We can define a utility function as a measure of gain or loss resulting from a decision being taken with regard to patient data and the states of nature, i.e. model parameters. When determining the optimal dosage regimen, given the observed patient data and a particular set of PK-PD parameters, a utility function measures the desirability of having chosen a particular dosage regimen [68].

In terms of a population PK-PD analysis, the utility function is specified in a way that the dosage regimens with the most favourable response and the lowest rates of adverse events (i.e. the optimal dosage regimens) have maximal values of the utility function [67, 68]. In other words, the utility is maximal when the optimal decision about the dosing regimen with regard to the predictive distribution of the individual's PK-PD parameters or response is made [68, 69].

2. AIM OF THE STUDY

Antibiotics are widely used in neonates. However, they are mostly not licenced in this population and the dose is not labelled.

In order to assure safe and effective treatment of infants optimal dose regimen has to be established. For time-dependent antimicrobials, such as β-lactam antibiotic meropenem, the percentage of dosing interval when plasma drug concentration is above minimal inhibitory concentration (MIC) is the best predictor of clinical efficiency.

In this study we will include data from 19 preterm neonates. They were treated with meropenem for mostly sepsis in neonatal hospital units in Tartu and Tallinn, both in Estonia. To nine of them the antibiotic was administered over 30 minutes and the rest ten subjects were given a 4-hour infusion.

Firstly, a population pharmacokinetic model for meropenem in neonates will be developed. Secondly, an optimization of infusion time using utility function will be performed. For the optimization we will use the final pharmacokinetic model and the distribution of MICs from EUCAST database for *E. coli*. The dose will be fixed to standard off-label dose of 20 mg/kg and target set to 100% of time above MIC. Based on this target, pharmacokinetic parameters, and MIC values an optimal infusion time will be determined. Pharmacokinetic modelling and infusion length optimization will be performed with non-linear mixed effects model software NONMEM.

The aim of this study is to determine at which infusion length meropenem concentration is the maximal percentage of time above MIC. It is expected that our study will contribute to the establishment of optimal dosing regimen for meropenem in neonates.

3. METHODS

3.1 SUBJECTS

This was a prospective open-label two-centre study performed in Estonia. It included 19 premature newborns (7 females and 12 males) with very low birth weight. Neonates were in neonatal intensive care units of Tartu University Hospital and Tallinn Children's hospital. The majority of them were severely ill and treated for several diseases, mostly sepsis [70].

Infants were given injectable antibiotic meropenem, diluted in 0.9% sodium chloride to a concentration of 10 mg/mL at a dose of 20 mg/kg every 12 hours. In 9 patients the antibiotic was given over 30 minutes and in 10 subjects over four hours. Six blood samples per patient were taken. Blood samples were collected (in Estonia) at steady state just before the administration, and then 0.5, 1.5, 4, 8 and 12 hours after the initiation of the infusion of the drug [70]. During the study the following items were recorded: time of blood sampling, meropenem dose, the infusion length, plasma concentration of meropenem, subject's weight, and age (GA, PNA, and PMA).

Meropenem plasma concentrations were measured in Estonian lab using Ultra High Pressure Liquid Chromatography (UHPLC) [70].

3.2 POPULATION PHARMACOKINETIC MODELLING

3.2.1 Population PK structural model

The data were modelled using the non-linear mixed effects model computer program (NONMEM) [52], allowing us to develop a complete PPK model, including average PK parameters, covariates and within- and between-subject variability. The plasma concentration versus time data from all patients were fitted simultaneously.

Several model files were tested in order to describe the data the best. The PPK model was built gradually, step by step. We started by defining the PK structural model. One- and two-

compartment models were evaluated as the basic PK model. A one-compartment model is represented by Equation 3.1. Equations 3.2 describe a two-compartment model.

$$k = \frac{CL}{V} \qquad\qquad \text{(Eq. 3.1)}$$

$$k = \frac{CL}{V1} \qquad k_{12} = \frac{Q}{V1} \quad k_{21} = \frac{Q}{V2} \qquad \text{(Eqs. 3.2)}$$

where k is the elimination rate constant, CL is clearance, V is volume of distribution, $V1$ represents V in compartment 1 (i.e. central compartment), and $V2$ in compartment 2 (i.e. peripheral compartment), Q is the inter-compartmental clearance (between compartment 1 and 2), k_{12} and k_{21} represent the rate of transfer from central to peripheral compartment and back, respectively.

3.2.2   *Population parameter estimates*

We obtained population PK parameter estimates using subroutine for one-compartment IV administration of meropenem. The subroutine (which is a routine that predicts the observed experimental result, using NONMEM's built-in differential equation solver [50]) used was ADVAN1 TRANS1 of NONMEM version VII, level 1.2.

Estimation method that was used was a FOCE method with η - ε interaction, i.e. interaction between interindividual and residual variability (`METHOD=1 INTER`). Maximal allowable number of evaluations of the objective function during the estimation step was set to 9999 (`MAXEVAL=9999`). The number of significant digits required in the final parameter estimate was by default three.

The covariance step was also incorporated into the PK model. During this step SEs of NONMEM parameters were calculated. A covariance between two elements, for example between clearance (*CL*) and volume of distribution (*V*), is a measure of statistical association between these two variables. Their covariance relates to their correlation (*r*), i.e.

$$r = \frac{covariance}{\sqrt{\omega_{CL} \times \omega_V}} \qquad \text{(Eq. 3.3)}$$

In order to describe WSV, i.e. the difference between observed and predicted concentration for an individual, two different error models were tested. At first we modelled the WSV with a combination of additive and proportional (or constant coefficient of variation) residual error model (Equation 3.4). After that, in order to describe residual variability, we also evaluated just the proportional error model (Equation 3.5).

$$C_{(obs)\,ij} = C_{ij} \times \left(1 + \varepsilon_{(prop)ij}\right) + \varepsilon_{(add)ij} \qquad \text{(Eq. 3.4)}$$

$$C_{(obs)\,ij} = C_{ij} \times \left(1 + \varepsilon_{ij}\right) \qquad \text{(Eq. 3.5)}$$

where $C_{(obs)ij}$ is the jth observed/measured serum concentration for the ith subject, C_{ij} represents the "true value" of $C_{(obs)ij}$, meaning it is the corresponding predicted serum concentration, ε_{ij} is the residual variability term, representing normally distributed random variable with a zero mean and variance σ^2.

To characterize BSV in the PK model parameters, an exponential variance model (Equation 3.6) was used. This model assumes a log-normal distribution of the variability and cannot go negative, since exp $(-\infty)$ is 0.

$$P_{ij} = P'_j \times e^{\eta_{ij}} \qquad \text{(Eq. 3.6)}$$

where P'_j represents population mean (i.e. the "typical value" in the population) for the jth parameter, P_{ij} represents the individual jth parameter for subject i, and η_{ij} is an independently distributed random variable with mean of zero and a variance of ω^2.

3.2.3   Covariates and scaling for size

The influence of body weight and age, specifically PMA, of the studied neonates on the different PK parameters were studied.

The apparent volume of distribution for meropenem is a function of growth. Thus, the

typical volume of distribution (V_{typ}) was scaled to size. For that we used an allometric model with PWR of 1 (Equation 3.7).

$$V_{typ} = V_{std} \times \frac{WT}{70} \qquad \text{(Eq. 3.7)}$$

where V_{std} is the typical volume of distribution for an adult weighing 70 kg (which is the adult median body weight) and WT is body weight in kilograms of the subject in the study.

The elimination clearance of meropenem was established to be dependent on growth and maturation of the neonates and their renal function. Growth was taken into account through an allometric model. In this case PWR was fixed to 0.632, a value from a published study from Rhodin et al [24] (Equation 3.8).

$$CL_{typ} = CL_{std} \times \left(\frac{WT}{70}\right)^{0.632} \times MF \qquad \text{(Eq. 3.8)}$$

where CL_{std} is the typical clearance for an adult whose body weight is 70 kg, WT is body weight in kilograms, and MF represents the maturation function.

Maturation of GFR and thus consequently the maturation of meropenem CL was integrated through previously described Hill equation or general hyperbolic maturation equation (Eq. 1.3). The values for Hill coefficient (3.33) and the PMA when clearance reaches 50% of its maximal value, i.e. T_{50} (55.4), were based on the empirical model of renal clearance from Rhodin et al [24]. Maturation of meropenem clearance was modelled according to maturation function (MF) shown in Equation 3.9.

$$MF = \frac{PMA^{3.33}}{55.4^{3.33} + PMA^{3.33}} \qquad \text{(Eq. 3.9)}$$

3.3 PK MODEL DISCRIMINATION AND EVALUATION

3.3.1   The discrimination between PK models

Statistical comparison of PK structural models was made using the likelihood ratio test, which is based on the minimum objective function value (OFV) output by NONMEM. The OFV is approximately minus two times the logarithm of the likelihood of the data. The difference in OFV is thus asymptotically χ^2-distributed. Differences in OFV of >3.84, >6.63 and >10.83 correspond to nominal significance levels of <0.05, <0.01 and <0.001 (1 degree of freedom), respectively [71, 72].

For a more complex model to be accepted, a lower value of OFV was required, when comparing to a model with the same number of parameters.

3.3.2   The evaluation of the PK model

The prediction power of the PK model, i.e. how well the final PK model estimates the population and individual predicted plasma concentrations, was tested through a non-compartmental analysis. The area under the curve ($AUC_{(0-t)}$) was calculated using software R [73] version 2.14.1, with the use of trapezoidal rule. From results we calculated prediction error (*PE*) (Equation 3.10) and relative PE (*RPE*) (Equation 3.11).

$$PE = OBS - PRED \qquad\qquad \text{(Eq. 3.10)}$$

$$RPE = \frac{OBS - PRED}{PRED} \qquad\qquad \text{(Eq. 3.11)}$$

where *OBS* are the observed values and *PRED* are the model predicted values.

The quality of fit of the PK model to the plasma concentration versus time data was sought through different evaluation techniques. In order to test the reliability of the conclusions or final estimates of the final PK model we used various tools for visual diagnostic, such as GOF plots (DV vs. PRED, DV vs. IPRED, CWRES vs. time, CWRES vs. PRED). Distribution of CWRES was also investigated.

With the purpose of revealing PK model misspecifications, VPC and pcVPC were performed by simulation of one thousand datasets using the original data.

In the case of pcVPC the observed and simulated concentration were normalised, i.e. prediction corrected for the differences within a single bin coming from variations in independent variables. Equation 3.12 represents prediction-corrected observation/prediction (pcY_{ij}):

$$pcY_{ij} = Y_{ij} \times \frac{\widetilde{PRED}_{bin}}{PRED_{ij}} \qquad \text{(Eq. 3.12)}$$

where Y_{ij} is the observed/predicted concentration for the ith individual and jth time point, $PRED_{ij}$ represents typical population prediction, and $\widetilde{PRED}_{bin}$ is the median of the typical population predictions for a specific bin of independent variables [61].

Once the prediction correction was done, the statistics were calculated. For every dataset (simulated and observed) and in each bin the median of the dependent variable was calculated in the same way. Out of the 1,000 median values for each bin from the simulations, a nonparametric 95% CI was calculated, i.e. the 2.5th and the 97.5th percentile. The results were then plotted against time and the median of the observed parameters was compared to the distribution of the simulated parameters.

To generate computations for VPCs and pcVPCs software PsN (Perl speaks NONMEM [74, 75]) in conjunction with NONMEM was used. Graphical presentation of the PsN output was done with R (version 2.14.1) [73] using package Xpose (version 4.3.2) [76-78].

To describe the reliability of the final PK model, we calculated relative standard errors (*RSE*) from standard errors (*SE*) (Equation 3.13). SE were estimated during the covariance step in NONMEM.

$$\% \, RSE = \frac{SE}{mean \, (population \, estimate)} \times 100\% \qquad \text{(Eq. 3.13)}$$

3.4 OPTIMIZATION OF THE INFUSION TIME

Using several evaluation techniques to define the adequacy of the final PK model helped

us to choose the best PK model. This model was then used for the optimization of the infusion length for meropenem. The methodology of the optimization comprised four successive steps: the preparation of the dataset, assignment of PK parameters and MIC values, and finally the optimization of the infusion time.

3.4.1 Preparation of the dataset

To prepare the dataset for the utility function, we selected subjects with desired demographics, which were GA less than 32 weeks and PNA less or equal to 2 weeks. Only 6 out of 19 subjects from this study met these requirements. In order to increase the sample size to 1,000 subjects, we added realistic demographic data (ages and body weight) for premature neonates from a neonatal database.

3.4.2 Assigning the pharmacokinetic parameters

One thousand subjects were assigned the PK parameters, i.e. V and CL using the final PPK model with NONMEM. After the simulation every subject had its own individual volume of distribution and individual clearance.

3.4.3 Assigning the MIC values

Afterwards the individual MIC values were assigned with R software. The discrete distribution of the MIC values was obtained from EUCAST MIC distributions [79] for *Escherichia coli* (*E. coli*) [80] (Figure 3.1 and Table 3.1). At the end, the distribution of the MIC values in the dataset of 1,000 subjects was random and followed the one from EUCAST.
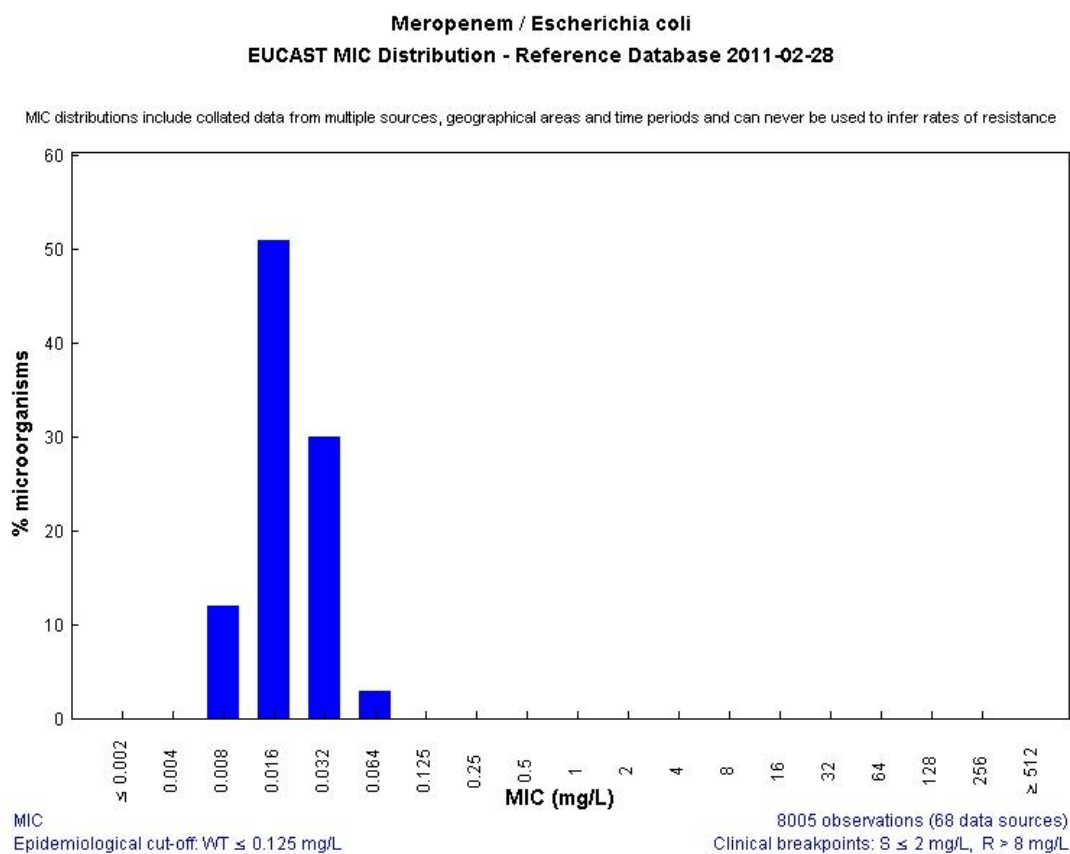
Figure 3.1: EUCAST meropenem MIC distribution for *Escherichia coli*; from [80]

Table 3.1: EUCAST meropenem MIC distribution for *Escherichia coli* from 8005 observations (68 data sources); from [80]

MIC (mg/L)	No. of observations with a specific MIC	Proportion of observations
0.002	0	0
0.004	0	0
0.008	999	0.125
0.016	4128	0.516
0.032	2449	0.306
0.064	288	0.0360
0.125	76	0.009496
0.25	41	0.005126
0.5	12	0.00150
1	8	0.00100
2	1	0.000125
4	1	0.000125
8	1	0.000125
16	1	0.000125
32	0	0
64	0	0
128	0	0
256	0	0
512	0	0

3.4.4   Utility function

Last step was the optimization of infusion time. This was done in NONMEM, using utility function. We wanted to identify the infusion time, for which the maximum utility would be achieved, i.e. the optimal infusion time. Development of the utility function derived from a study by Viberg et al [65]. Fixed dose of 20 mg per kg of body weight (usual off-label dose for meropenem in neonates [38]) was used. Meropenem is an antibiotic that exhibits time-dependent killing, thus the aim was to get as close to 100% T>MIC as possible. We used the Hill equation with a high value of the sigmoidicity coefficient (`GAM=99`), which approximately dichotomized the results. Estimation method used was FOCE, the minimal number of significant digits was by default three and the subroutine used was ADVAN6.

3.4.5   Visual presentation of the results

Results of the optimization of infusion time were inspected by several plots. Optimal infusion time versus MIC value was used to illustrate how the optimal infusion time changes with growing MIC value. To find outliers, plot of individual OFV (iOFV) versus ID number was made. We fixed θ (infusion time) each time to a different number, made multiple NONMEM runs, and looked at how OFV changes. Using these results we made a plot of OFV vs. infusion time (for MIC of 2 mg/L), which is basically log-likelihood profiling. We also made box plots with T>MIC on y-axis and MIC value or optimal infusion length on the x-axis. The latter was done using MIC of 2 and 8 mg/L, the susceptibility and resistance breakpoints for *E. coli*. Percentage of subjects whose T>MIC is less than 40% versus infusion time at MIC of 2 and 8 mg/L was also investigated. Plots were made with custom R-scripts.

4. RESULTS

4.1 SUBJECTS

Nineteen premature neonates were enrolled into the study. Nine of them were given infusion of meropenem over 30 minutes and ten of them over four hours. A total of 114 observations were collected for the analysis. Characteristics of the studied neonates are shown in Tables 4.1 and 4.2. The mean (standard deviation (SD)) body weight was 977 (208) g, GA was 26.7 (1.6) weeks, and PNA 2.6 (1.1) weeks.

Table 4.1: Individual demographic data of the subjects included in the study

ID	WT (g)	GA (weeks)	PNA (weeks)	PMA (weeks)
1	846	26.43	3.14	29.57
2	1190	26.00	4.71	30.71
3	1295	28.00	2.14	30.14
4	930	28.71	0.57	29.28
5	875	28.00	2.00	30.00
6	670	24.86	1.00	25.86
7	570	27.86	1.43	29.29
8	1470	28.00	2.57	30.57
9	1015	27.43	2.43	29.86
10	1100	30.14	1.71	31.86
11	890	24.57	3.43	28.00
12	835	25.00	2.86	27.86
13	1080	26.43	4.00	30.43
14	845	24.71	2.14	26.85
15	1040	25.00	3.00	28.00
16	1000	28.00	4.57	32.57
17	885	24.71	1.86	26.57
18	1080	26.29	2.29	28.58
19	940	26.43	3.43	29.86

ID is subject's ID number, WT is body weight, GA is gestational age, PNA postnatal age, and PMA postmenstrual age

Table 4.2: Summarized statistics of the demographic features of the subjects used for the development of the pharmacokinetic model

	min	max	mean	SD
WT (g)	570	1470	977	208
GA (weeks)	24.57	30.14	26.66	1.62
PNA (weeks)	0.57	4.71	2.59	1.12
PMA (weeks)	25.86	32.57	29.25	1.75

ID is subject's ID number, WT is body weight, GA is gestational age, PNA postnatal age, and PMA postmenstrual age

For the optimization of the infusion length we used one thousand subjects. Their mean (SD) weight was 1284 (300) g, GA 28.8 (1.6) weeks, and PNA 0.5 (0.5) weeks (Table 4.3).

Table 4.3: Summarized statistics of the demographic features of the subjects used for the optimization of infusion time

	min	max	mean	SD
WT (g)	570	1940	1284	300
GA (weeks)	24.71	31.00	28.79	1.55
PNA (weeks)	0.14	2.00	0.53	0.52
PMA (weeks)	25.86	32.29	29.32	1.50

ID is subject's ID number, WT is body weight, GA is gestational age, PNA postnatal age, and PMA postmenstrual age

Raw plots, illustrating observed plasma concentration-time curves for all 19 subjects, are presented in Figures 4.1 and 4.2. In Figure 4.1 one subject's (ID=15) maximum plasma concentration was observed at 8 hours, although its infusion duration was 4 hours. Other subjects had expected PK profiles. In Figure 4.2 the mean observed plasma concentration-time profile is plotted, and the difference between the two dosing regimens is clearly seen.
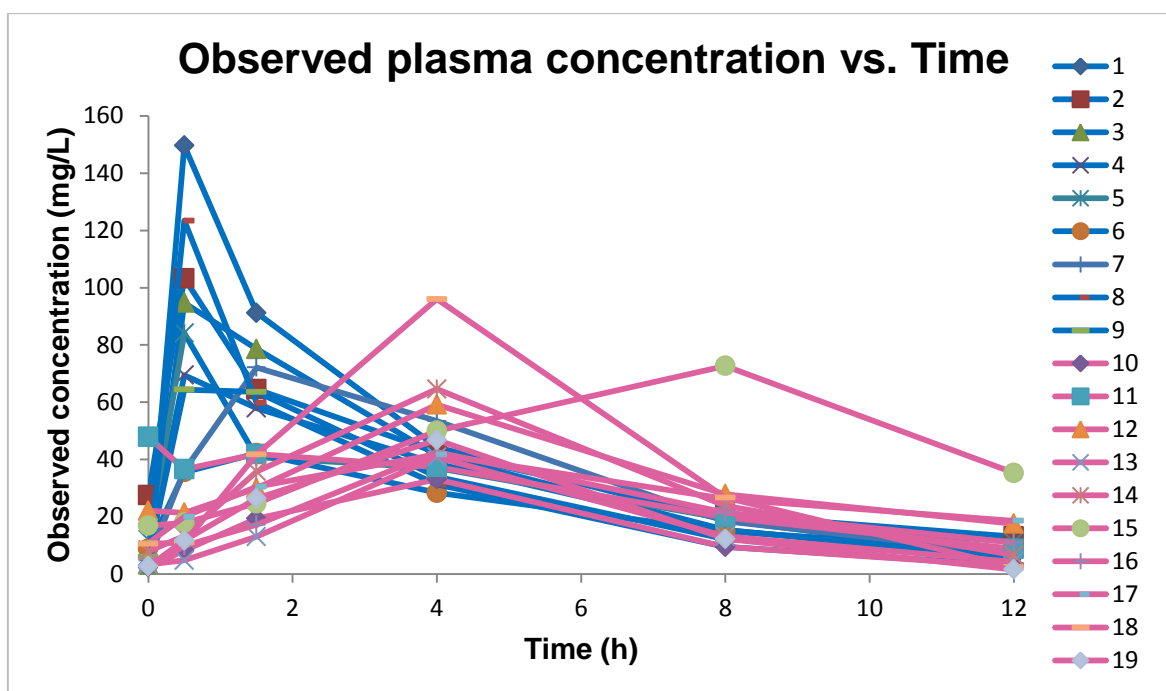
Figure 4.1: Observed individual plasma concentration versus time; each line indicates an individual subject; blue lines represent subjects with half an hour infusion; violet lines represent subjects with four hour infusion; dots indicate sampling times
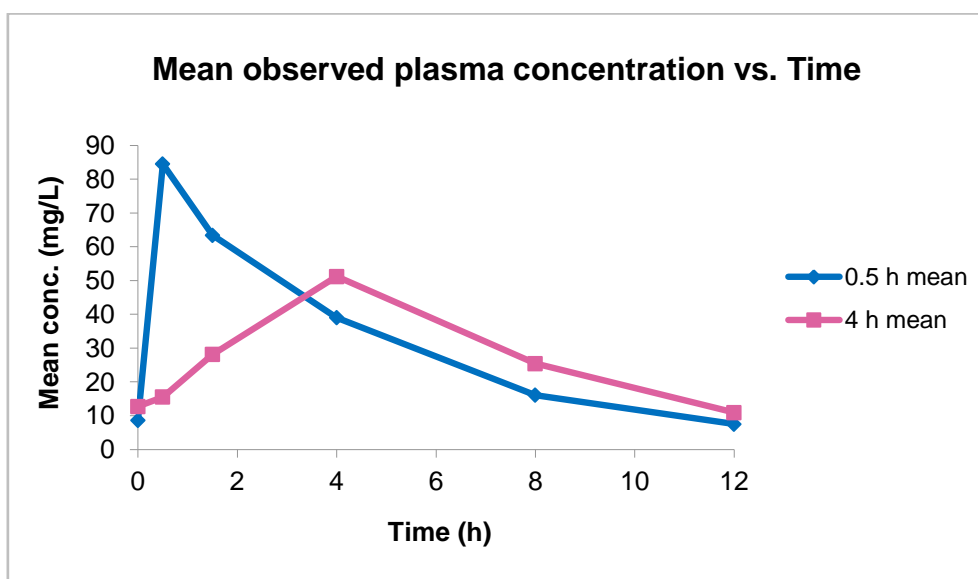

Figure 4.2: Mean observed plasma concentration versus time; each line indicates a specific pharmacokinetic profile; blue line represents subjects with 30-minute infusion and violet line the subjects with 4-hour infusion; dots indicate sampling times

4.2 POPULATION PHARMACOKINETIC MODELLING

The base PK model was a 1-compartment model (for IV administration), which provided almost the same OFV as a 2-compartment model when using the same number of PK parameters. Between the combination of additive and proportional residual error model and just the proportional model, the latter one showed no zero gradients and proved to be better to describe WSV. BSV in model parameters was modelled by an exponential variance model.

The final covariate PK model for meropenem PK in neonates provided a better fit to the observed data then the base model. Comparing to the base PK model in the covariate model meropenem CL was allometrically scaled by body weight with PWR of 0.632 and additionally with the maturation function. The T_{50} value and Hill coefficient were fixed to 55.4 and 3.33, respectively. These values originated from empirical model of renal clearance from Rhodin et al [24]. The V in the final covariate model was scaled proportionally to body weight.

The following equations (Equations 4.1 and 4.2) represented the final model:

$$CL = \theta_{CL} \times \left(\frac{WT}{70}\right)^{0.632} \times \frac{PMA^{3.33}}{55.4^{3.33}+PMA^{3.33}} \times e^{\eta_{CL}} \qquad \text{(Eq. 4.1)}$$

$$V = \theta_V \times \left(\frac{WT}{70}\right) \times e^{\eta_V} \qquad \text{(Eq. 4.2)}$$

where *CL* and *V* are PK parameters in individual subject, *PMA* is the postmenstrual age in weeks, *WT* is the body weight in kg, and η_{CL} and η_V describe random deviations of individual subjects' parameters from the typical value in adult population (θ_{CL} and θ_V).

The base PK model provided the following PK parameters: typical value of CL was estimated at 0.06 L/h (with RSE of 8.58%) and V at 0.28 L (with RSE of 10.21%). BSV of CL and V were 38.73% and 34.64%, respectively. Residual error was 30.59%.

The OFV for the final model with covariates was approximately 7.4 units lower than the OFV for the base PK model. The changes in OFV and BSV after addition of the covariates

(body weight and age, specifically PMA) to the base model are shown in Table 4.4. The BSV on CL was lower in the final model (it dropped from 38.7% to 30.3%), whereas there was no improvement in the BSV on V.

Table 4.4: Change in objective function value (OFV) and between-subject variability (BSV) before and after the addition of covariates into the model

Model	OFV	Δ OFV	BSV (%)
Base model	610.939		
TVCL = THETA(1)			38.73
TVV = THETA(2)			34.64
Final covariate model	603.565	7.374	
TVCL = THETA(1)*MF*(WTKG/70)**(0.632)			30.33
TVV = THETA(2)*(WTKG/70)			34.93

TVCL is the typical value of clearance, TVV the typical value of volume of distribution, MF is the maturation function, WTKG is body weight in kilograms, THETA is the estimated parameter

The values of the final parameter estimates from NONMEM are given in Table 4.5. CL was estimated at 7.95 L/h/70kg (with RSE of 6.81%) and V at 20.7 L/70kg (with RSE of 10.14%).

Table 4.5: NONMEM results – final parameter estimates, standard errors (SE), relative standard errors (RSE) and 95% confidence interval (CI)

	mean	SE	RSE (%)	95% CI
Fixed effects				
Clearance (L/h)	7.95	0.5410	6.81	6.89 – 9.01
Volume of distribution (L)	20.7	2.1000	10.14	16.58 – 24.82
T50 [fixed] (weeks)	55.4			
Hill coefficient [fixed]	3.33			
Random effects				
BSV on CL (%)	30.33	0.0277	30.11	20.00 – 38.73
BSV on V (%)	34.93	0.0381	31.23	22.36 – 44.72
Random/residual error				
WSV; proportional error (%)	30.53	0.0227	24.36	22.36 – 37.42

T_{50} represents the postmenstrual age when clearance reaches 50% of adult value, Hill coefficient is the sigmoidicity coefficient in the Hill equation, BSV is between-subject variability, WSV is within-subject variability, CL is meropenem clearance, and V is meropenem volume of distribution. T_{50} and Hill coefficient were fixed to a number from a published study on renal function maturation [24], therefore standard errors were not calculated for these two parameters.

4.3 EVALUATION OF THE PHARMACOKINETIC MODEL

Non-compartmental analysis provided the following results (Table 4.6): mean (SD) $AUC_{(0-t)}$ calculated using trapezoidal rule was 338.6 (48.1) mg.h/L for PRED and 350.8 (95.1) mg.h/L for IPRED, comparing to 364.7 (100.1) mg/L calculated from the observed plasma concentrations. The median relative prediction error (RPE) for PRED was 7.9% and 7.0% for IPRED. Figures 4.3 and 4.4 illustrate the fit of AUC, calculated from predicted (AUCpred) and individual predicted (AUCipred) plasma concentrations, to AUC values, calculated from the observed plasma concentrations (AUCobs).

Table 4.6: Comparison of areas under the curve ($AUC_{(0-t)}$) from non-compartmental analysis of observed, predicted and individual predicted concentration data with prediction errors

ID	AUCobs	Population prediction			Individual prediction		
		AUC40pred	PE	RPE (%)	AUC40ipred	IPE	RIPE (%)
1	503.2	307.8	195.4	63.5	432.2	70.9	16.4
2	437.9	318.8	119.1	37.3	486.3	-48.4	-9.9
3	415.9	331.9	84.0	25.3	357.4	58.5	16.4
4	353.0	353.4	-0.4	-0.1	332.8	20.2	6.1
5	354.3	325.3	29.0	8.9	365.6	-11.3	-3.1
6	269.3	429.3	-160.1	-37.3	280.7	-11.5	-4.1
7	415.3	281.1	134.2	47.7	360.2	55.0	15.3
8	343.3	318.2	25.0	7.9	323.3	20.0	6.2
9	331.9	332.6	-0.7	-0.2	310.3	21.6	7.0
10	191.2	315.4	-124.2	-39.4	195.5	-4.3	-2.2
11	319.1	368.5	-49.4	-13.4	510.0	-190.9	-37.4
12	407.8	366.8	41.0	11.2	394.6	13.2	3.3
13	220.5	301.8	-81.2	-26.9	202.0	18.5	9.1
14	391.0	405.5	-14.6	-3.6	338.9	52.0	15.4
15	580.6	352.8	227.7	64.5	529.9	50.6	9.5
16	283.9	237.3	46.6	19.6	254.5	29.4	11.6
17	346.6	431.5	-84.9	-19.7	352.7	-6.1	-1.7
18	505.0	342.5	162.5	47.5	400.2	104.8	26.2
19	259.5	313.3	-53.8	-17.2	238.9	20.6	8.6
mean	364.7	338.6	26.1	9.2	350.8	13.8	4.9
median	353.0	331.9	25.0	7.9	352.7	20.2	7.0
SD	100.1	48.1	107.6	31.9	95.1	60.7	13.5

AUCobs represents the area under the curve calculated from observed meropenem concentrations, AUCpred is calculated from predicted, and AUCipred from individual predicted concentrations. PE is prediction error for population predictions, RPE is relative PE, IPE is prediction error for individual predictions, and RIPE is relative IPE.
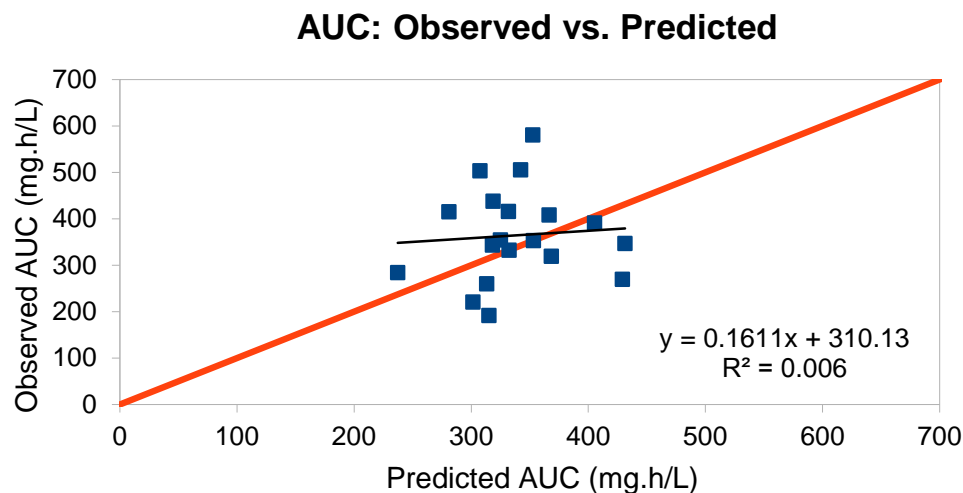
AUC: Observed vs. Predicted

Figure 4.3: Areas under the curve calculated from observed vs. population predicted concentrations; the red line is the line of unity (y=x), blue thin line is linear regression
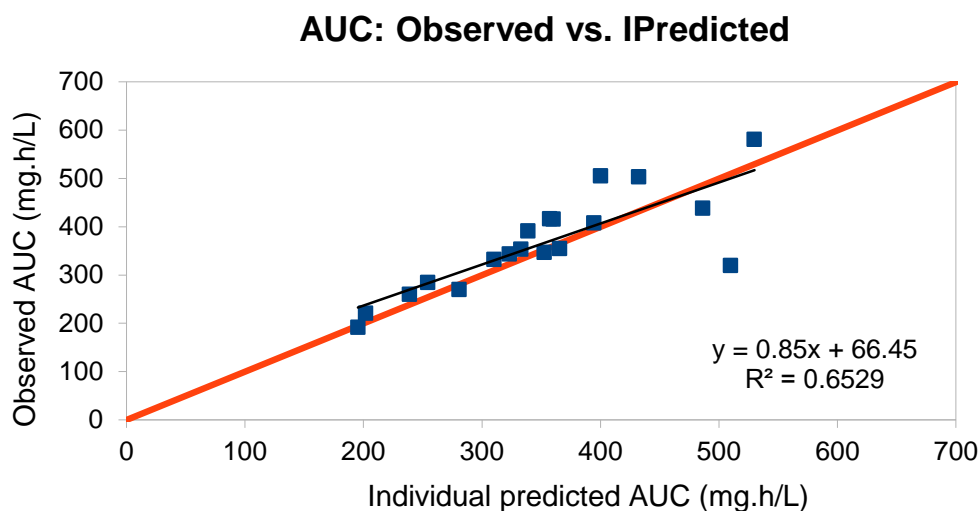
AUC: Observed vs. IPredicted

Figure 4.4: Areas under the curve calculated from observed vs. individual predicted concentrations; the red line is the line of unity (y=x), blue thin line is linear regression

Individual plots (Figure 4.5) demonstrate how good the population and individual prediction of the final model was for each individual subject. Subjects with ID numbers from 1 to 9 were given half an hour infusion, and those from 10 to 19 got four hour infusion. On the individual level, the model captured the concentration quite well; however there was some underprediction in subject with ID no. 1, 2, 5, 8 and 18. And in subject, whose ID is 6, there was some population overprediction.
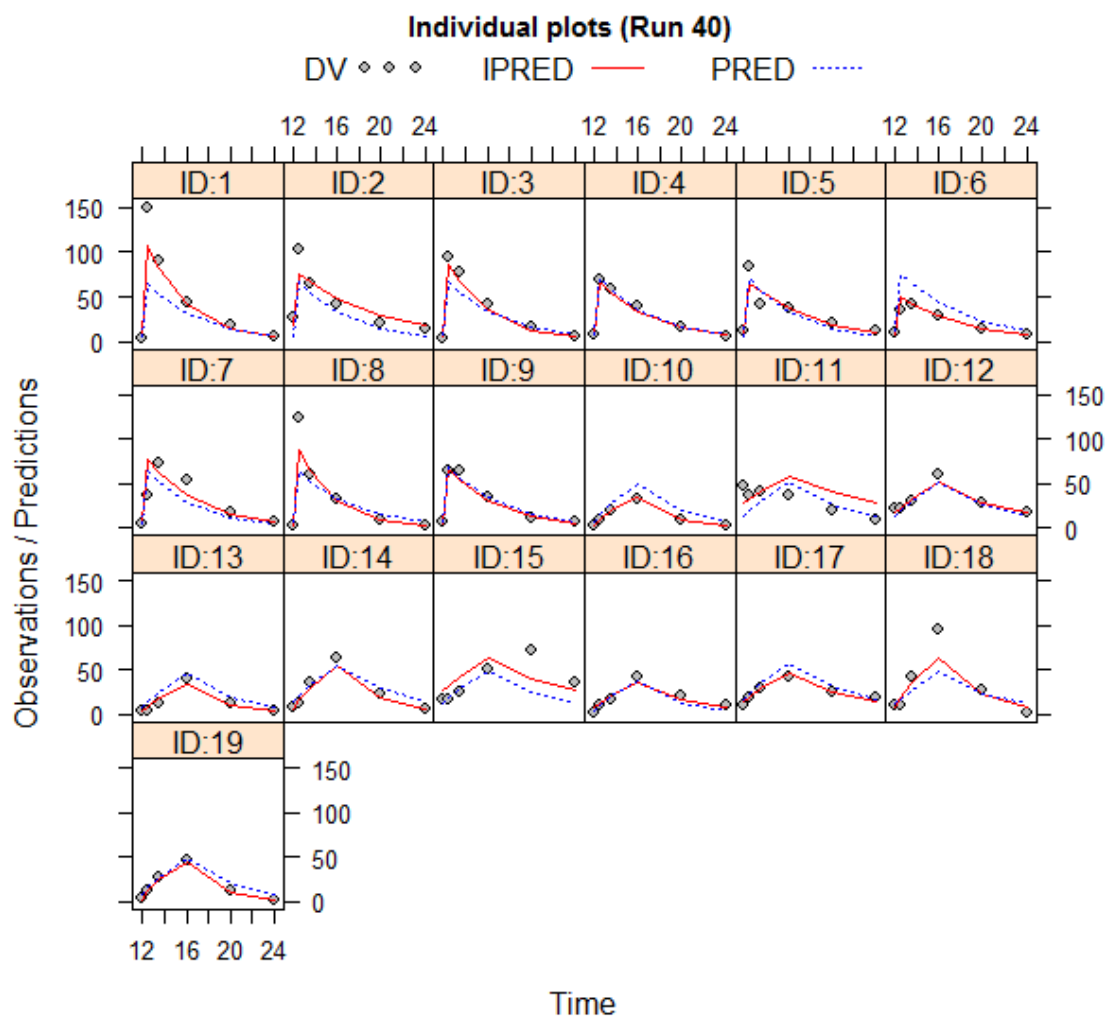
Figure 4.5: Concentration-time plots for each individual subject. Grey dots represent the observed concentration, blue dashed line is the population predicted concentration and the red solid line is the individual predicted concentration.

Some of diagnostic GOF plots (DV versus PRED and IPRED) are shown in Figure 4.6. All the data points are uniformly distributed along the line of identity and there is no bias seen. In the case of DV vs. IPRED the points are closer to the line of unity than in the case of DV vs. PRED. In the log-log graphs we can see the distribution of the data points around the line of unity better than in normal scale and we can confirm the uniform distribution of the points on either side of lines of identity.

DV vs. PRED

a)

DV vs. IPRED

b)

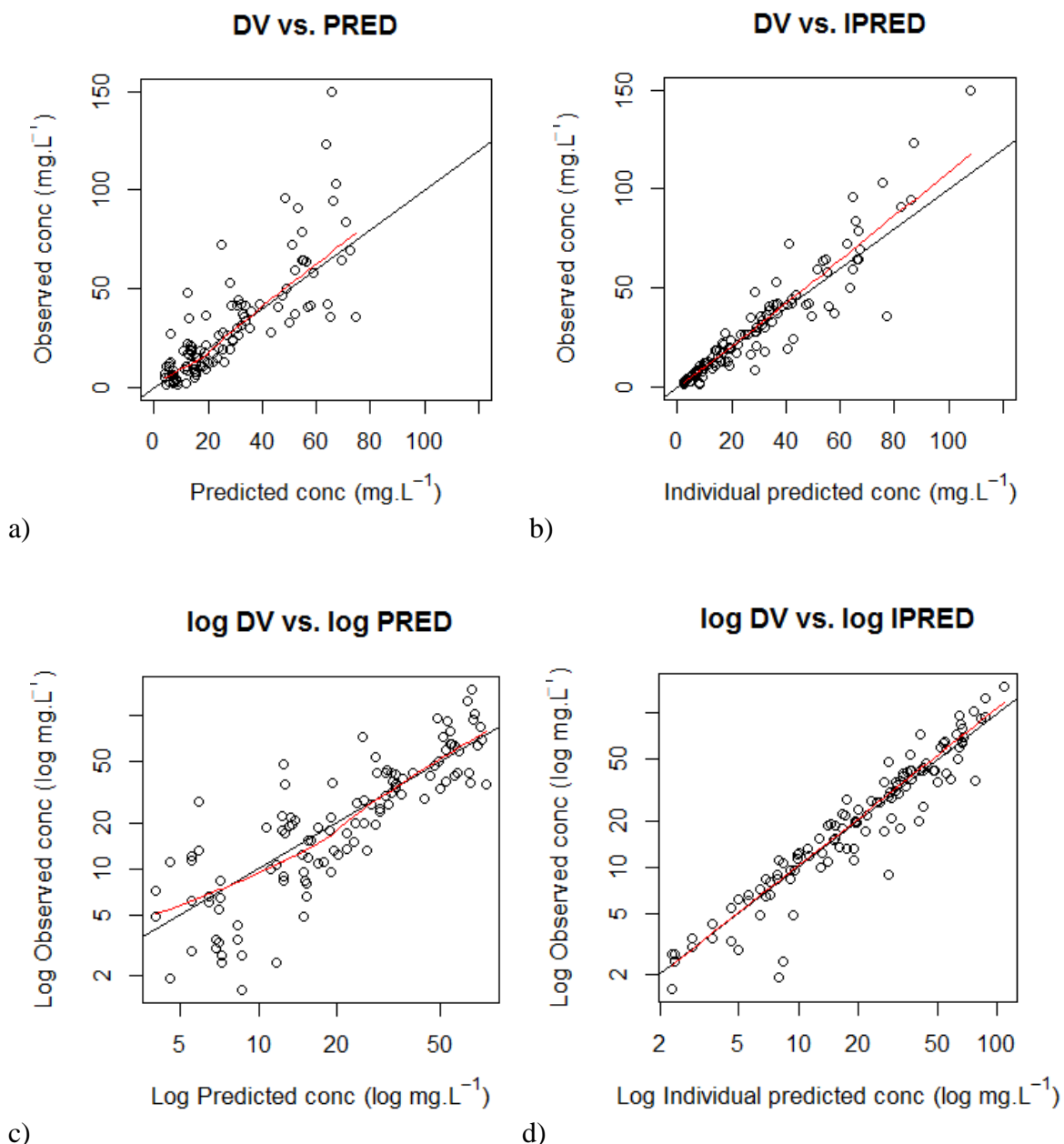## log DV vs. log PRED

c)

log DV vs. log IPRED

d)

Figure 4.6: Observed (DV) versus a) population predicted (PRED) and b) individual predicted (IPRED) concentration; and on a logarithmic scale: logarithmic values of observed concentrations versus c) log PRED and d) log IPRED. Black solid line is the line of unity and red solid line is a lowess line.

Figure 4.7 illustrates another type of GOF plots, residual plots, showing CWRES versus time and versus PRED. On both plots the majority, 95% of the points, lie between 2 and -2 and the lowess line is almost trendless, there is almost no deviation from the line of y equals 0. Also, the data points are homogenously distributed on both sides of the line y=0. On the plots of distribution of CWRES (Figure 4.8) it can be seen that CWRES are

36

normally distributed.
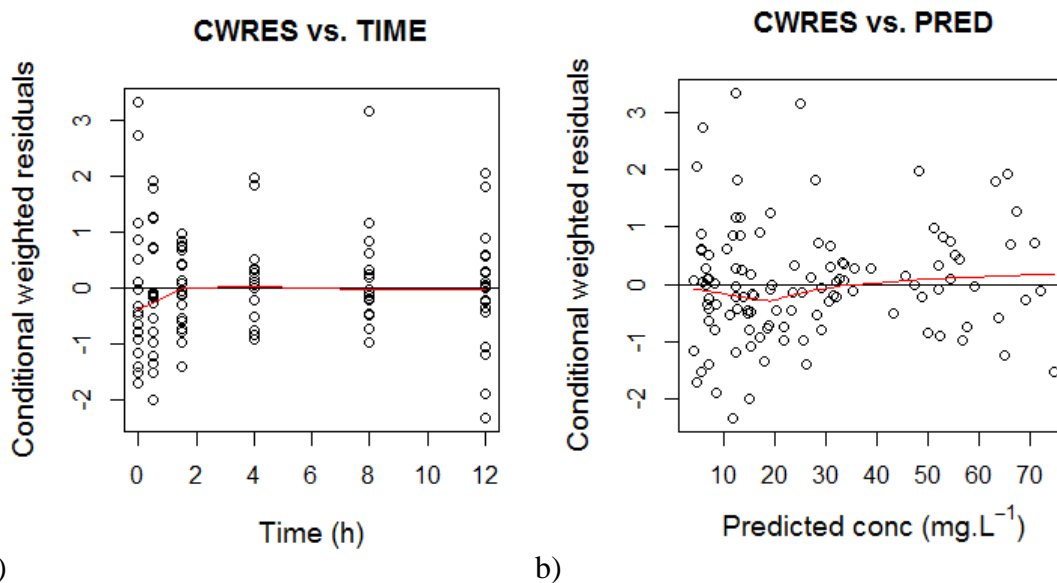
a)   b)

Figure 4.7: Conditional weighted residuals (CWRES) versus a) time and b) population predictions (PRED). Solid red line is a lowess line.
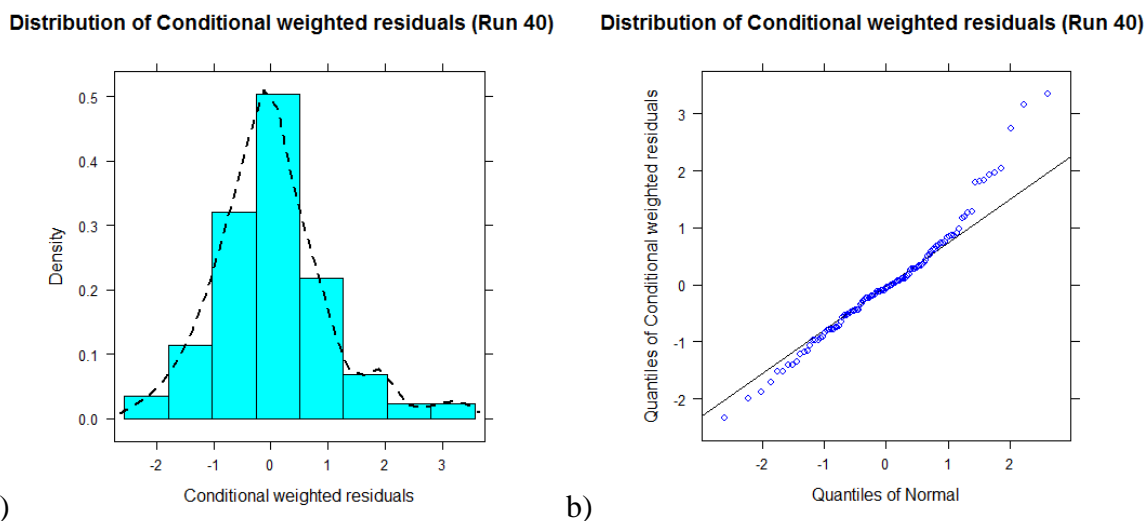
a)   b)

Figure 4.8: Distribution of conditional weighted residuals (CWRES); a) a histogram, showing the density of the CWRES distribution, and b) a normal q – q plot of CWRES

A VPC and pcVPC for the final covariate model are presented in Figure 4.9. The line that represents the median of the observed concentration lies within the nonparametric 95% confidence interval of the model predicted median. Neither traditional VPC nor pcVPC indicated any important misspecification of the final PK model.

Figure 4.9: a) Visual predictive check (VPC), b) Prediction-corrected VPC; 1,000 simulated datasets were simulated for this plot; blue dots represent the observed concentration; shad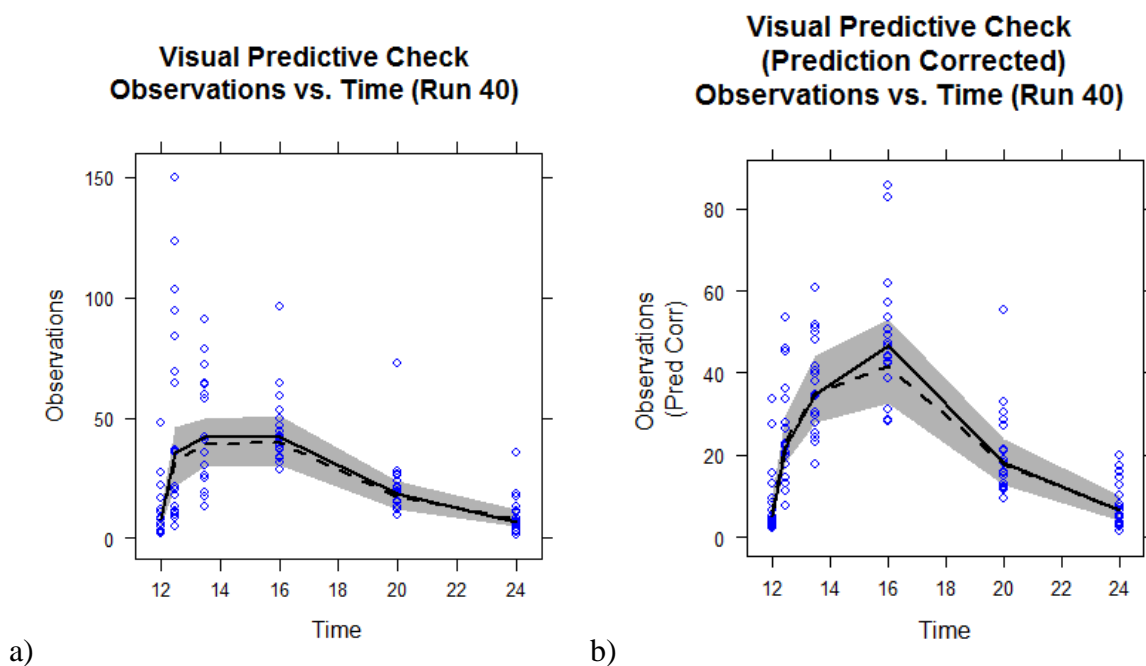ed grey area is the nonparametric 95% confidence interval of the predicted median; black solid line is the median of the observed data; black dashed line is the median of the simulated data

4.4 OPTIMIZATION OF THE INFUSION TIME

When we randomly assigned MIC values to 1,000 simulated subjects, the optimal infusion time that was determined by NONMEM differed a lot. There was a big influence of the subjects with outlying MIC values. Figures 4.10-12 show scatter plots of individual OFV (iOFV) versus subject's ID number. In Figure 4.10 and 4.11 the MIC distribution in the subjects was nonparametric and followed the one from EUCAST database. Figure 4.10 demonstrates a distribution where the maximum MIC was 2 mg/L, and in Figure 4.11 the maximum MIC was 16 mg/L. Final estimations of the optimal infusion time were 0.99 hours in the first case and 10.5 hours in the second. Figure 4.12 shows the plot where we set the MIC values for all subjects to MIC of 2 mg/L. On this plot there are no subjects with outlying iOFV values seen. Optimal infusion length in this case was estimated at 6.07 hours.

Figure 4.10: Individual OFV (iOFV) versus subject's ID number; each dot represents a subject in the optimization; MIC values are assigned randomly, according to distribution from EUCAST database for *E. coli*; the outliers are subjects with ID (MIC in mg/L) 8 (2), 16 (1), 431 (1), 777 (0.5).
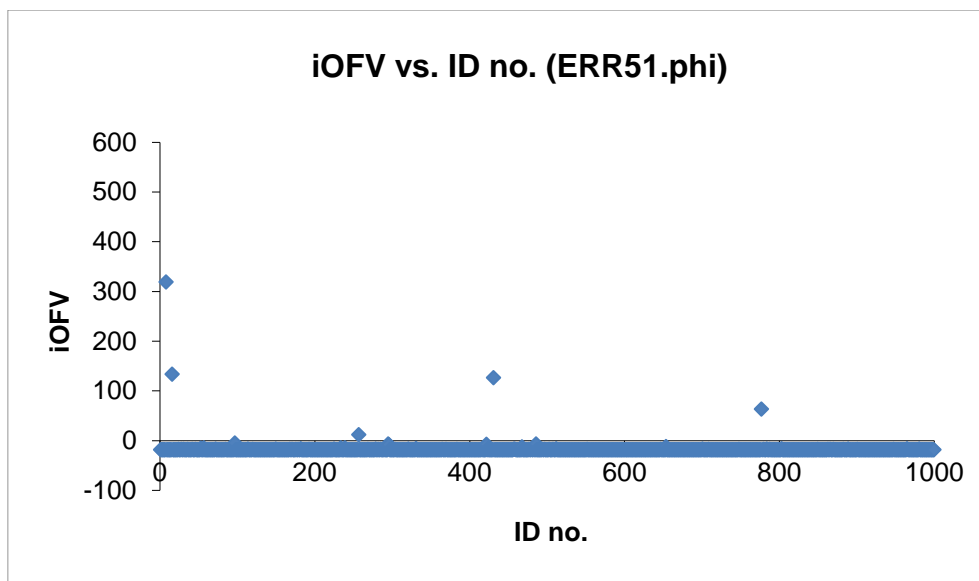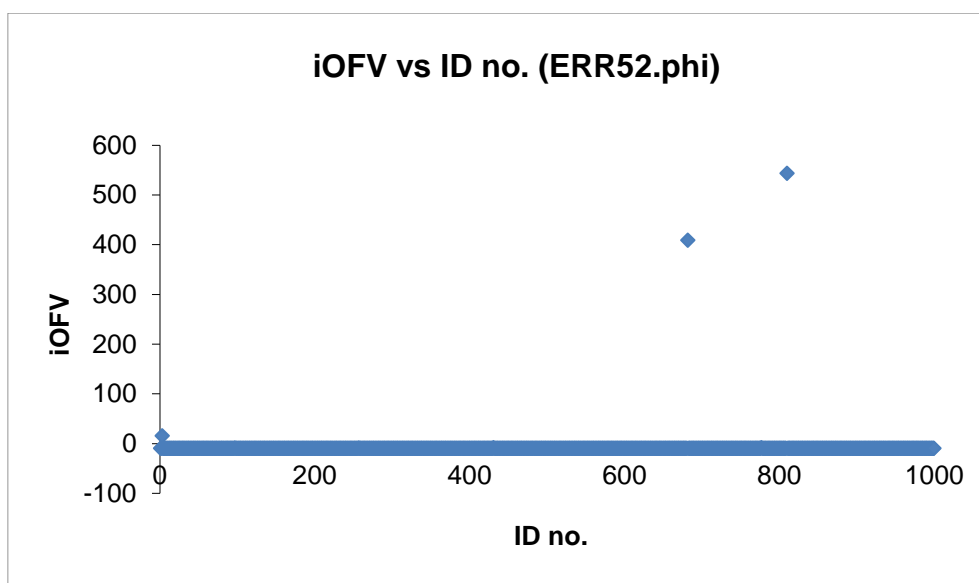

Figure 4.11: Individual OFV (iOFV) versus subject's ID number; each dot represents a subject in the optimization; MIC values are assigned randomly, according to distribution from EUCAST database for *E. coli*; the outliers are subjects with ID (MIC in mg/L) 682 (8), 810 (16).
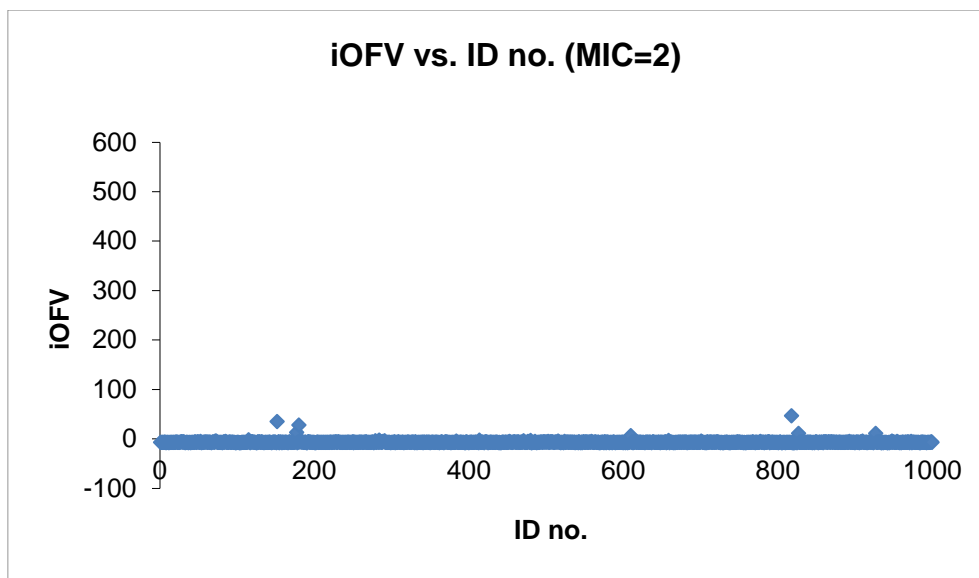
Figure 4.12: Individual OFV (iOFV) versus subject's ID number; each dot represents a subject in the optimization; MICs for all subjects are set to 2 mg/L

Figure 4.13 demonstrates how the estimated optimal infusion time changes with increasing MIC values. In each NONMEM run MIC values were set to a different value. From MIC of 0.08 to 2 mg/L, the optimal infusion length steeply increased from 0.08 h, which is less than 5 minutes, to 6 hours. Then it rose more gradually. For MIC of 2 mg/L, which is the susceptibility breakpoint for *E. coli*, and for MIC of 8 mg/L, which is the resistance breakpoint for the same microorganism, estimated optimal infusion time for meropenem was 6.07 hours and 6.98 hours, respectively. From MIC of 11 mg/L, the optimal infusion time began to decrease again to practically a bolus injection at MIC of 25 mg/L.

Optimal infusion time vs. MIC value
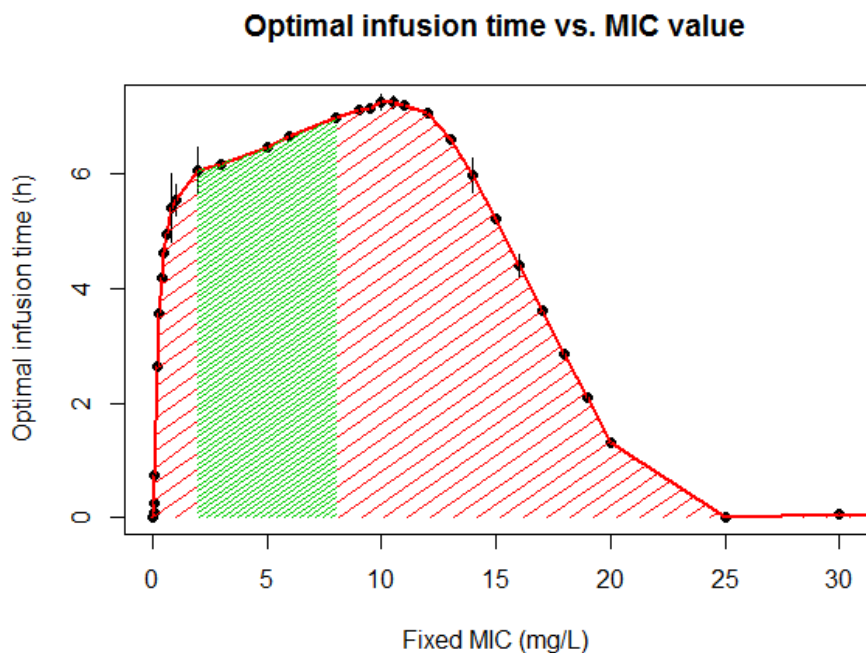
Figure 4.13: Optimal infusion time for meropenem versus MIC value; vertical black lines demonstrate the standard error; green area represents MIC from 2 to 8 mg/L, the susceptibility and resistance breakpoints for *E. coli*

Plot of OFV versus optimal infusion time for meropenem, with MIC values for all subjects fixed to 2 mg/L, is illustrated in Figure 4.14. From the plot we see that the minimum OFV (-6853.37) matches the optimal infusion time determined by NONMEM (6.07 hours).
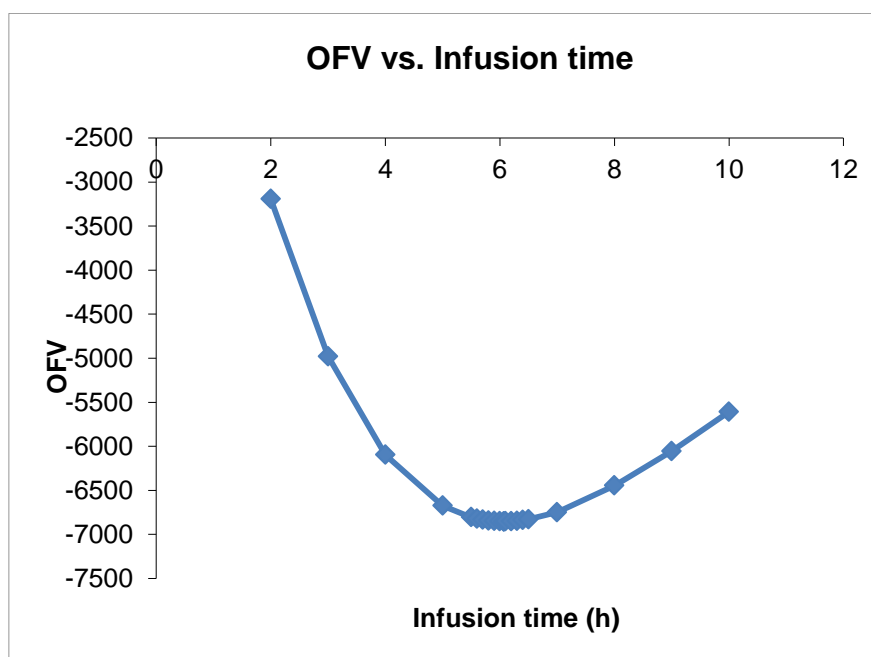
Figure 4.14: Objective function value (OFV) versus infusion time

Figure 4.15 illustrates box-and-whisker plots of T>MIC versus MIC value. We can see that by increasing MIC value, T>MIC is decreasing: when MIC is 0.08 mg/L, T>MIC is approximately 100%, for MIC of 2 mg/L, median T>MIC is around 98%; when MIC value is 8 mg/L, median T>MIC is between 90 and 95%, and for MIC of 16 mg/L, median T>MIC is approximately 70-75%.
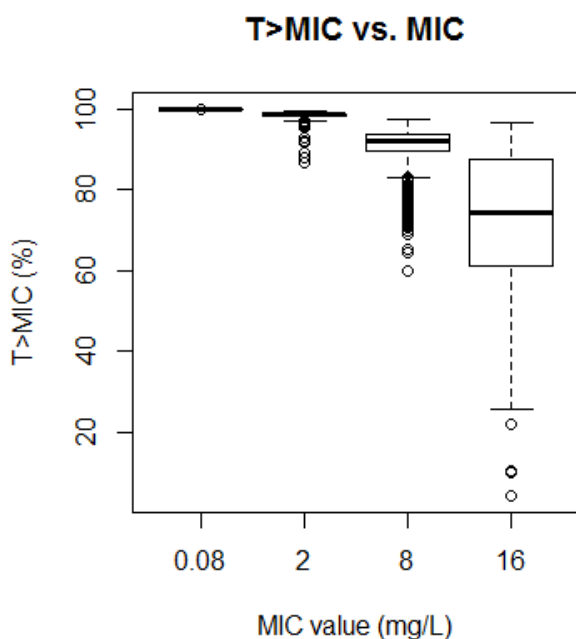
Figure 4.15: Percentage of dosing interval with meropenem concentration above MIC (T>MIC) versus MIC value; the box represents the 25th, 50th and 75th percentile, the whiskers the highest and lowest value, and the dots the outliers

The plot of T>MIC versus infusion time for *E. coli* susceptibility and resistance breakpoints, MIC of 2 and 8 mg/L, respectively, is shown in Figure 4.16. When MIC was set to 2 mg/L, the median T>MIC was approximately 100% for every infusion time. The T>MIC was lower in the second case, when MIC was set to 8 mg/L; the median was around 95% for all infusion times. Infusion times were set to realistic times, such as bolus IV injection, 30-minute, and 1, 2, 4 and 6-hour infusion.
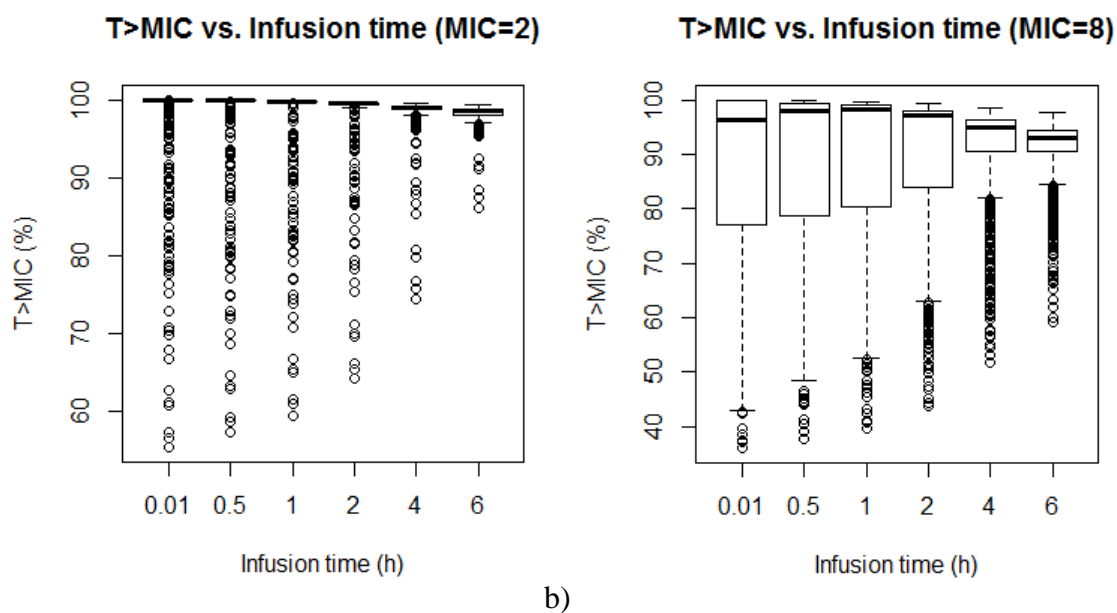
Figure 4.16: Percentage of dosing interval with meropenem concentration above MIC (T>MIC) versus infusion time for MIC of a) 2 mg/L and b) 8 mg/L, the susceptibility and resistance breakpoints for *E. coli*; the box represents the 25th, 50th and 75th percentile, the whiskers the highest and lowest value, and the dots the outliers

In Figure 4.17 it can be seen what percentage of subjects had their T>MIC lower than 40% and how this changes when we increase the infusion length. For *E. coli* susceptibility breakpoint for meropenem, all subjects had their T>MIC bigger than 40%. When MIC was set to 8 mg/L, the percentage of subjects whose T>MIC is lower than 40% was higher than in the first case, however, it was never above 1%. The highest percentage (approximately 0.6%) was in the case of bolus IV injection. In the case of a 1-hour infusion it fell to around 0.1% and for 2-, 4-, and 6-hour infusion the percentage of subjects with T>MIC lower than 40% was 0.

Figure 4.17: Percentage of subjects with fraction of dosing interval when meropenem concentration is above MIC (T>MIC) lower than 40% versus infusion time for MIC of a) 2 mg/L and b) 8 mg/L, the susceptibility and resistance breakpoints for *E. coli*

5. DISCUSSION

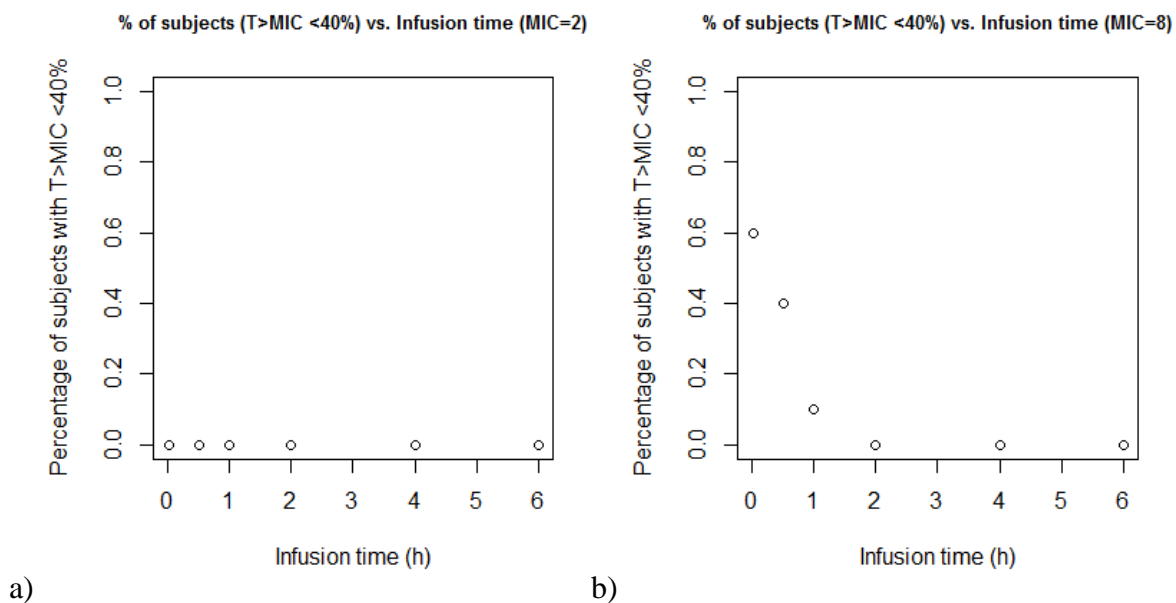We studied pharmacokinetics of β-lactam antibiotic meropenem in neonates and developed a population pharmacokinetic model, which we afterwards used to optimize infusion time for meropenem.

Data from nineteen preborn neonates were collected. Nine of these neonates were given infusion over half an hour and ten of them over four hours. Infusion of meropenem was given intravenously every 12 hours and plasma concentration of it was measured at steady state just before the administration, and 0.5 h (to get the maximal plasma concentration (c_{max}) for meropenem in patients with a 30-minute infusion), 1.5 h, 4 h (to get meropenem c_{max} for subjects with a 4-hour infusion), 6 h and 12 h after the initiation of the infusion. All subjects seemed to follow their expected PK profile; given the rate of infusion they were given. However, one subject, who was given a 4-hour infusion, did not have c_{max} 4 h after the start of the infusion. This might as well be a measuring error.

The data from premature neonates were modelled with non-linear mixed effects software NONMEM. The final structural PPK model was a 1-compartment model, since a 2-compartment model produced almost exactly the same OFV value, indicating that it had collapsed to a 1-compartment one. Proportional model proved to be better for modelling the WSV than a combination of proportional and additive error model. There were no zero gradients seen in the first error model and it provided a better fit to the data. Exponential model was chosen for modelling BSV.
The incorporation of covariates (body weight and PMA) into the model improved the fit to the data. Meropenem is predominantly excreted by kidneys. Especially for drugs eliminated via this route it was proposed to use only size and maturation as a base for dosing regimen. Since in preterm neonates the predictions of creatinine production rate has not yet been well established, and its use for predicting GFR is thus discouraged in this population [13]. Consequently, serum creatinine was not used as a covariate. In the final model V and CL were scaled with allometric function with PWR of 1 and 0.632, respectively. This way differences in body size were accounted for. As renal CL in addition

to size depends on maturation of GFR as well, a maturation function was used too. The values of coefficient in the sigmoid hyperbolic Hill equation were fixed to a value from a published study of human renal function maturation [24]. Hill coefficient used was 3.33 and T_{50} value was 55.4.

The OFV was as expected lower in the final covariate model, comparing to the base PK model. The addition of covariates improved the BSV for almost 8.5% as well.

The values of the final parameter estimates from NONMEM for an adult with an average weight of 70 kg were (RSE): CL was estimated at 7.95 L/h (6.81%) and V at 20.7 L (10.14%). In literature the values for meropenem CL and V for an adult were approximately 11-18 L/h [25, 26] and 12.5-23 L [25-27], respectively. Compared to literature values, meropenem CL was lower. One of the reasons for this might be that the maturation function did not capture it properly. Maybe this happened because in premature infants it can take even up to 8 years to achieve adult GFR values [11]. Or we might have achieved better results if we tried to estimate Hill coefficient and T_{50} value, instead of fixing them. But due to small sample size of our study these parameters could not have been estimated. On the other hand, V for meropenem estimated by NONMEM lied within the ranges, reported in literature, showing that allometric scaling with exponent of 1 was adequate.

To evaluate the final PK model several techniques and diagnostic plots were used. Reliability of the model was proven by a relatively small RSE; for typical values of PK parameters it was within 10% and RSE of random effects was 24%. A non-compartmental analysis showed that the model predictions of $AUC_{(0-t)}$ were unbiased, as median RPE for AUCs calculated from population predicted meropenem concentrations was 7.9% and median RPE for AUCs calculated from individual predicted concentration was 7.0%.

Individual plots of observed, population predicted and individual predicted concentrations versus time showed some under- and overprediction, but overall, the model predicted the concentrations quite well. Goodness-of-fit plots confirmed that the final PK model is appropriate. In scatter plot DV versus PRED or IPRED the points were uniformly distributed on either side of line of identity, meaning that the predictions match the observations. There was also no bias seen in the predictions. As expected the plot of DV

vs. IPRED was better than DV vs. PRED as IPRED also includes the unexplained interindividual variability. On both residual plots, CWRES vs. time and vs. PRED, CWRES were homogenously distributed between -2 and 2, and the lowess line was almost trendless. This confirmed that there is almost no unaccounted heterogeneity in the data and that the structural PK model was adequate.

Additionally, the traditional and prediction-corrected VPC of the final model also showed that the PK model had satisfactory predictive performance as the median of observed concentrations lay within the nonparametric 95% CI of the simulated median. Due to the small dataset size other prediction intervals (PI), such as PI for the 5th and 95th percentile, were not examined.

Several diagnostic plots corroborated the adequacy of the final PK model to predict the concentrations of meropenem, so this model was later on used for the optimization of the infusion length. Optimization was done with the use of utility function, which derived from a previous study [65]. When MIC distribution in the simulated dataset of 1,000 subjects was random and followed the one from EUCAST database (for *E. coli*), there were substantial differences in the estimated optimal infusion time. Upon further investigation it was established that only subjects with much higher MIC values than the rest, influenced the estimated infusion length. These outlying subjects had individual OFV (iOFV) [81, 82] well above the iOFV for the majority of subjects. For example, the majority had iOFV around 0, and one of those influential subjects had iOFV of 500. This of course resulted in a different estimation of infusion time, as only a few higher iOFVs contributed a lot to the total OFV. For instance, in the dataset where the maximal MIC was 2 mg/L the optimal infusion time was estimated to be almost 1 h, whereas if the maximal MIC was 16 mg/L, it was over 10 h. Discovering this, we decided to assign all the subjects the same MIC value as oppose to follow the one from EUCAST distribution.

Subjects with low iOFV had the most frequent MIC value from the EUCAST distribution, 0.016 mg/L. With MIC value so low the length of the infusion is almost irrelevant as the concentration of meropenem is almost always above MIC. This is probably the reason for low iOFV values and why they are not significant when estimating the infusion time.

Setting the MIC values for all subjects to the same number proved that iOFV really is dependent on MIC value, as in this case there were no individuals with iOFV much higher

than the rest.

Plot of optimal infusion time versus fixed MIC value showed that with an increase in MIC to 2 mg/L infusion time at first drastically increased (to approximately 6 h). After that, in the range of MICs between 2 and 11 mg/L it rose more steadily (to around 7 h at 11 mg/L) and with additional increase in MIC, it steeply fell again. We can see this trend because at the end, when the MIC values get bigger, the only way that meropenem c_{max} can reach MIC is if it is given as a bolus IV injection.

Plotting OFV versus fixed infusion time was performed to see if the defined infusion length is really the one with the smallest OFV. NONMEM was not optimizing the infusion time in this case and the MIC values were fixed as well. The plot confirmed that the estimated optimal infusion time is really associated with the global minimum of OFV.

Box-and-whisker plots of T>MIC versus MIC value showed that when MIC value is low (0.08 and 2 mg/L), meropenem concentration is practically all the time above MIC. And even with MIC set to 16 mg/L, the median T>MIC was approximately 70%, which is well above the threshold for bacteriostatic and bactericidal effect for meropenem (20 and 40%, respectively [37, 42]).

Optimal infusion time for MIC of 2 mg/L (*E. coli* susceptibility breakpoint for meropenem) was estimated at 6 hours. However, box plots of T>MIC vs. infusion time show that if we give meropenem as a bolus IV injection, the median T>MIC is still almost 100% and if the antibiotic is given over 30 minutes, or 1, 2, 4 or 6 hours, the median T>MIC is always above 95%. None of the subjects with MIC set to 2 mg/L had T>MIC lower than 40%, meaning that meropenem would have bactericidal activity.

For *E. coli* resistance breakpoint (8 mg/L) the optimal infusion time estimated by the use of utility function in NONMEM was 7 hours. Still, given as a bolus injection, the 25th percentile of T>MIC would be approximately 75% and the median T>MIC above 95%. Only some outliers had their T>MIC lower than approximately 43%, which is still above 40% and thus enough for meropenem bactericidal effect. Even when infusion is given over shorter period of time (bolus IV, 0.5, 1, 2, 4, and 6 hours) meropenem is bactericidal, as the percentage of subjects with T>MIC lower than 40% never gets above 1%.

From these results we can deduct that although the optimal infusion length for meropenem in neonates with MICs for all subjects set to 2 and 8 mg/L (*E. coli* susceptibility and resistance breakpoints) is 6 and 7 hours, respectively, we still get satisfactory fraction of time above MIC even if we give the antibiotic as a bolus injection or a short infusion.

6. CONCLUSION

A population pharmacokinetic model for meropenem in preterm neonates was developed. The final model which provided the best fit to the plasma concentration-time data was a 1-compartment model with proportional error model and between-subject variability modelled with exponential model. Physiological parameterisation for clearance was used. Final estimates of meropenem pharmacokinetic parameters were: clearance was 7.95 L/h/70kg and volume of distribution 20.7 L/70kg, with 30.33% and 34.93% between-subject variability, respectively.

The final population pharmacokinetic model was used for optimization of infusion length. When MIC values from EUCAST distribution for *Escherichia coli* were randomly assigned, there was no single optimal infusion time; due to influential individuals with high MIC values. By setting MIC values to *E. coli* susceptibility (2 mg/L) and resistance (8 mg/L) breakpoints the optimal infusion times were approximately 6 and 7 hours, respectively. Visual inspection of the results revealed that even shorter infusion lengths, such as bolus IV injection, 30-minute, 1-, 2-, and 4-hour infusion were sufficient for bacteriostatic and even bactericidal activity of meropenem. Based on these results we can conclude that for infections in neonates, caused by microorganisms with resistance breakpoint of 8 mg/L or lower, it is not expected that antimicrobial efficacy of meropenem would be influenced by infusion time.

The optimization of infusion length was done with *E. coli* EUCAST distribution. However, the model can be useful for other bacteria as well, since a lot of them have their susceptibility and resistance breakpoints at 2 and 8 mg/L, respectively. And even if the microorganism has different breakpoints than *E. coli* the model could be easily adjusted.

Although population pharmacokinetic models cannot replace carefully designed clinical studies, they are especially useful in paediatric population, where the postnatal development is rapid. Rapid development combined with maturation complicate the preparation of a classical clinical study, resulting in not many drugs being thoroughly *in vivo* evaluated in this population.

7. REFERENCES

1. ICH, *Harmonised tripartite guideline. Clinical investigation of medicinal products in the pediatric population*, in *International Conference on Harmonisation of Technical Requirements for Registration of Pharmaceuticals for Human Use, 20 July 2000*.

2. Foreman, S.W., K.A. Thomas, and S.T. Blackburn, *Individual and gender differences matter in preterm infant state development.* J Obstet Gynecol Neonatal Nurs, 2008. **37**(6): 657-65.

3. Strolin Benedetti, M. and E.L. Baltes, *Drug metabolism and disposition in children.* Fundam Clin Pharmacol, 2003. **17**(3): 281-99.

4. Alcorn, J. and P.J. McNamara, *Pharmacokinetics in the newborn.* Adv Drug Deliv Rev, 2003. **55**(5): 667-86.

5. Vetterly, C.G. and D.L. Howrie, *A Pharmacokinetic and Pharmacodynamic Review*, in *Critical Care of Children with Heart Disease*, R. Munoz, et al., Editors. 2010, Springer London. 83-87.

6. Routledge, P.A., *Pharmacokinetics in children.* J Antimicrob Chemother, 1994. **34 Suppl A**: 19-24.

7. Kearns, G.L., et al., *Developmental pharmacology--drug disposition, action, and therapy in infants and children.* N Engl J Med, 2003. **349**(12): 1157-67.

8. Howrie, D. and C. Schmitt, *Clinical Pharmacokinetics: Applications in Pediatric Practice*, in *Handbook of Pediatric Cardiovascular Drugs*, R. Munoz, et al., Editors. 2008, Springer London. 17-32.

9. Anker, J.N., M. Schwab, and G.L. Kearns, *Developmental Pharmacokinetics*, in *Pediatric Clinical Pharmacology*, H.W. Seyberth, A. Rane, and M. Schwab, Editors. 2011, Springer Berlin Heidelberg. 51-75.

10. Alcorn, J. and P.J. McNamara, *Ontogeny of hepatic and renal systemic clearance pathways in infants: part I.* Clin Pharmacokinet, 2002. **41**(12): 959-98.

11. Solhaug, M.J., P.M. Bolger, and P.A. Jose, *The developing kidney and environmental toxins.* Pediatrics, 2004. **113**(4 Suppl): 1084-91.

12. Engle, W.A., *Age terminology during the perinatal period.* Pediatrics, 2004. **114**(5): 1362-4.

13.   Anderson, B.J. and N.H. Holford, *Mechanistic basis of using body size and maturation to predict clearance in humans.* Drug Metab Pharmacokinet, 2009. **24**(1): 25-36.

14.   Anderson, B.J. and N.H. Holford, *Mechanism-based concepts of size and maturity in pharmacokinetics.* Annu Rev Pharmacol Toxicol, 2008. **48**: 303-32.

15.   Alcorn, J. and P.J. McNamara, *Using ontogeny information to build predictive models for drug elimination.* Drug Discov Today, 2008. **13**(11-12): 507-12.

16.   West, G.B., J.H. Brown, and B.J. Enquist, *The fourth dimension of life: fractal geometry and allometric scaling of organisms.* Science, 1999. **284**(5420): 1677-9.

17.   West, G.B., J.H. Brown, and B.J. Enquist, *A general model for the origin of allometric scaling laws in biology.* Science, 1997. **276**(5309): 122-6.

18.   Mahmood, I., *Prediction of drug clearance in children from adults: a comparison of several allometric methods.* Br J Clin Pharmacol, 2006. **61**(5): 545-57.

19.   Knibbe, C., *Are Children Small Adults: What can modeling offer to (clinical) practice?*, in *PAGE 18 (2009) Abstr 1678 [www.page-meeting.org/?abstract=1678]*: St. Petersburg, Russia.

20.   Dodds, P.S., D.H. Rothman, and J.S. Weitz, *Re-examination of the "3/4-law" of metabolism.* J Theor Biol, 2001. **209**(1): 9-27.

21.   Hu, T.M. and W.L. Hayton, *Allometric scaling of xenobiotic clearance: uncertainty versus universality.* AAPS PharmSci, 2001. **3**(4): E29.

22.   Tod, M., V. Jullien, and G. Pons, *Facilitation of drug evaluation in children by population methods and modelling.* Clin Pharmacokinet, 2008. **47**(4): 231-43.

23.   Anderson, B.J. and P. Larsson, *A maturation model for midazolam clearance.* Paediatr Anaesth, 2011. **21**(3): 302-8.

24.   Rhodin, M.M., et al., *Human renal function maturation: a quantitative description using weight and postmenstrual age.* Pediatr Nephrol, 2009. **24**(1): 67-76.

25.   Moon, Y.S., K.C. Chung, and M.A. Gill, *Pharmacokinetics of meropenem in animals, healthy volunteers, and patients.* Clin Infect Dis, 1997. **24 Suppl 2**: S249-55.

26.   Blumer, J.L., *Meropenem: evaluation of a new generation carbapenem.* Int J Antimicrob Agents, 1997. **8**(2): 73-92.

27.   Craig, W.A., *The pharmacology of meropenem, a new carbapenem antibiotic.* Clin Infect Dis, 1997. **24 Suppl 2**: S266-75.

28. Drusano, G.L. and M. Hutchison, *The pharmacokinetics of meropenem.* Scand J Infect Dis Suppl, 1995. **96**: 11-6.

29. Mouton, J.W. and J.N. van den Anker, *Meropenem clinical pharmacokinetics.* Clin Pharmacokinet, 1995. **28**(4): 275-86.

30. Smith, B., et al., *Pharmacokinetics and safety of meropenem in young infants with intra-abdominal infections.* Early Hum Dev, 2009. **85**(10, Supplement): S96-S97.

31. van Enk, J.G., D.J. Touw, and H.N. Lafeber, *Pharmacokinetics of meropenem in preterm neonates.* Ther Drug Monit, 2001. **23**(3): 198-201.

32. Leroy, A., et al., *Pharmacokinetics of meropenem in subjects with renal insufficiency.* Eur J Clin Pharmacol, 1992. **42**(5): 535-8.

33. Muro, T., et al., *Population pharmacokinetic analysis of meropenem in Japanese adult patients.* J Clin Pharm Ther, 2011. **36**(2): 230-6.

34. Parker, E.M., M. Hutchison, and J.L. Blumer, *The pharmacokinetics of meropenem in infants and children: a population analysis.* J Antimicrob Chemother, 1995. **36 Suppl A**: 63-71.

35. Isla, A., et al., *Population pharmacokinetics of meropenem in critically ill patients undergoing continuous renal replacement therapy.* Clin Pharmacokinet, 2008. **47**(3): 173-80.

36. Christensson, B.A., et al., *Pharmacokinetics of meropenem in patients with cystic fibrosis.* Eur J Clin Microbiol Infect Dis, 1998. **17**(12): 873-6.

37. Nicolau, D.P., *Pharmacokinetic and pharmacodynamic properties of meropenem.* Clin Infect Dis, 2008. **47 Suppl 1**: S32-40.

38. Meronem, *Summary of Product Characteristics, AstraZeneca,* *http://www.medicines.org.uk/emc/medicine/11215/SPC/ (last accessed on 21.03.2012).*

39. Rho, J.P., *Principles of Antimicrobial Therapy*, in *Infectious Disease in the Aging*, D. Norman and T. Yoshikawa, Editors. 2009, Humana Press. 43-59.

40. Zhanel, G.G., et al., *Ertapenem: review of a new carbapenem.* Expert Rev Anti Infect Ther, 2005. **3**(1): 23-39.

41. Andrews, J.M., *Determination of minimum inhibitory concentrations.* J Antimicrob Chemother, 2001. **48 Suppl 1**: 5-16.

42. Drusano, G.L., *Antimicrobial pharmacodynamics: critical interactions of 'bug and drug'.* Nat Rev Micro, 2004. **2**(4): 289-300.

43. Craig, W.A., *Antimicrobial resistance issues of the future.* Diagn Microbiol Infect Dis, 1996. **25**(4): 213-7.

44. Shah, P.M., *Parenteral carbapenems.* Clin Microbiol Infect, 2008. **14 Suppl 1**: 175-80.

45. Merrem, *Prescribing Information for Merrem IV (meropenem for injection), AstraZeneca; http://www.merremiv.com/, last accessed 22.03.2012.*

46. EUCAST, *Clinical Breakpoint Table v. 2.0 2012-01-01, http://www.eucast.org/fileadmin/src/media/PDFs/EUCAST_files/Breakpoint_tables/ Breakpoint_table_v_2.0_120221.pdf, last accessed on 22.03.2012.*

47. Baldwin, C.M., K.A. Lyseng-Williamson, and S.J. Keam, *Meropenem: a review of its use in the treatment of serious bacterial infections.* Drugs, 2008. **68**(6): 803-38.

48. Ette, E.I. and P.J. Williams, *Population pharmacokinetics I: background, concepts, and models.* Ann Pharmacother, 2004. **38**(10): 1702-6.

49. Ette, E.I. and P.J. Williams, *Population pharmacokinetics II: estimation methods.* Ann Pharmacother, 2004. **38**(11): 1907-15.

50. Shafer, S., *Fisher/Shafer NONMEM Workshop: Pharmacokinetic and Pharmacodynamic Analysis with NONMEM; Basic Concepts*, 2007: Het Pand, Ghent, Belgium.

51. Anderson, B.J., G.A. Woollard, and N.H. Holford, *A model for size and age changes in the pharmacokinetics of paracetamol in neonates, infants and children.* Br J Clin Pharmacol, 2000. **50**(2): 125-34.

52. Boeckmann, A.J., S.L. Beal, and L.B. Sheiner, *NONMEM users guide*, 1999: University of California at San Francisco, San Francisco.

53. Ette, E.I., P.J. Williams, and J.R. Lane, *Population pharmacokinetics III: design, analysis, and application of population pharmacokinetic Studies.* Ann Pharmacother, 2004. **38**(12): 2136-44.

54. Karlsson, M.O. and R.M. Savic, *Diagnosing model diagnostics.* Clin Pharmacol Ther, 2007. **82**(1): 17-20.

55. Ette, E.I. and T.M. Ludden, *Population pharmacokinetic modeling: the importance of informative graphics.* Pharm Res, 1995. **12**(12): 1845-55.

56. Brendel, K., et al., *Are population pharmacokinetic and/or pharmacodynamic models adequately evaluated? A survey of the literature from 2002 to 2004.* Clin Pharmacokinet, 2007. **46**(3): 221-34.

57.   Hooker, A., C.E. Staatz, and M.O. Karlsson, *Conditional weighted residuals, an improved model diagnostic for the FO/FOCE methods*, in *PAGE 15 (2006) Abstr 1001 [www.page-meeting.org/?abstract=1001]:* Brugge/Bruges, Belgium.

58.   EMA and CHMP, *European Medicines Agency, Commitee for medicinal products for human use - Guideline on reporting the results of population pharmacokinetic analyses; [http://www.tga.gov.au/pdf/euguide/ewp18599006en.pdf]*, 2007: London, UK.

59.   Yano, Y., S.L. Beal, and L.B. Sheiner, *Evaluating pharmacokinetic/pharmacodynamic models using the posterior predictive check.* J Pharmacokinet Pharmacodyn, 2001. **28**(2): 171-92.

60.   Post, T.M., et al., *Extensions to the visual predictive check to facilitate model performance evaluation.* J Pharmacokinet Pharmacodyn, 2008. **35**(2): 185-202.

61.   Bergstrand, M., et al., *Prediction-corrected visual predictive checks for diagnosing nonlinear mixed-effects models.* AAPS J, 2011. **13**(2): 143-51.

62.   Karlsson, M.O. and N. Holford, *A Tutorial on Visual Predictive Checks*, in *PAGE 17 (2008) Abstr 1434 [www.page-meeting.org/?abstract=1434]:* Marseille, France.

63.   Holford, N.H., *The Visual Predictive Check – Superiority to Standard Diagnostic (Rorschach) Plots*, in *PAGE 14 (2005) Abstr 738 [www.page-meeting.org/?abstract=738]:* Pamplona, Spain.

64.   Wang, D.D. and S. Zhang, *Standardized Visual Predictive Check – How and When to used it in Model Evaluation*, in *PAGE 18 (2009) Abstr 1501 [www.page-meeting.org/?abstract=1501]:* St. Petersburg, Russia.

65.   Viberg, A., et al., *Estimation of cefuroxime dosage using pharmacodynamic targets, MIC distributions, and minimization of a risk function.* J Clin Pharmacol, 2008. **48**(11): 1270-81.

66.   Miller, R., et al., *The Strategic Role and Application of Pharmacokinetic/Pharmacodynamic Modeling in Drug Development*, in *Pharmacokinetics in Drug Development: Clinical study design and analysis*, P.L. Bonate and D.R. Howard, Editors. 2004. 572; (551-82).

67.   Ivanova, A., et al., *An adaptive design for identifying the dose with the best efficacy/tolerability profile with application to a crossover dose-finding study.* Stat Med, 2009. **28**(24): 2941-51.

68.   Graham, G., S. Gupta, and L. Aarons, *Determination of an optimal dosage regimen*

using a Bayesian decision analysis of efficacy and adverse effect data. J Pharmacokinet Pharmacodyn, 2002. **29**(1): 67-88.

69.   Sheiner, L.B., *PK/PD approach to dose selection.* International Congress Series, 2001. **1220**(0): 67-78.

70.   Padari, H., et al., *Population pharmacokinetics of meropenem in very low birth weight neonates; ESPID abstract*, 2011.

71.   Wahlby, U., et al., *Assessment of type I error rates for the statistical sub-model in NONMEM.* J Pharmacokinet Pharmacodyn, 2002. **29**(3): 251-69.

72.   Wahlby, U., E.N. Jonsson, and M.O. Karlsson, *Assessment of actual significance levels for covariate effects in NONMEM.* J Pharmacokinet Pharmacodyn, 2001. **28**(3): 231-52.

73.   *R: a language and environment for statistical computing; Available from: http://www.R-project.org; last accessed on 27.02.2012.*

74.   Lindbom, L., P. Pihlgren, and E.N. Jonsson, *PsN-Toolkit--a collection of computer intensive statistical methods for non-linear mixed effect modeling using NONMEM.* Comput Methods Programs Biomed, 2005. **79**(3): 241-57.

75.   Lindbom, L., J. Ribbing, and E.N. Jonsson, *Perl-speaks-NONMEM (PsN)--a Perl module for NONMEM related programming.* Comput Methods Programs Biomed, 2004. **75**(2): 85-94.

76.   Jonsson, E.N. and M.O. Karlsson, *Xpose--an S-PLUS based population pharmacokinetic/pharmacodynamic model building aid for NONMEM.* Comput Methods Programs Biomed, 1999. **58**(1): 51-64.

77.   Harling, K., et al., *Xpose and Perl speaks NONMEM (PsN)*, in *PAGE 19 (2010) Abstr 1842 [www.page-meeting.org/?abstract=1842]:* Berlin, Germany.

78.   Xpose. *http://xpose.sourceforge.net; last accessed 06.03.2012*.

79.   EUCAST, *Antimicrobial wild type distributions of microorganisms, http://mic.eucast.org/, last accessed on 29.02.2012*.

80.   EUCAST, *Data from the EUCAST MIC distribution website http://217.70.33.99/Eucast2/regShow.jsp?Id=5402, last accessed 28.02.2011*.

81.   Sadray, S., E.N. Jonsson, and M.O. Karlsson, *Likelihood-based diagnostics for influential individuals in non-linear mixed effects model selection.* Pharm Res, 1999. **16**(8): 1260-5.

82.   Carlsson, K.C., et al., *Mixture models in NONMEM; How to find the individual*

probability of belonging to a specific mixture, and why this can be useful information., in *PAGE 15 (2006) Abstr 956 [www.page-meeting.org/?abstract=956]:* Brugge/Bruges, Belgium.

8. FINAL POPULATION PHARMACOKINETIC MODEL FOR MEROPENEM

```
$PROBLEM MEROPENEM prop ERROR MODEL
      ;$PROBLEM specifies the title of the problem

$INPUT ID IDOR=DROP TIME AMT RATE WT DV EVID SS II GA PNA PMA CREA
      ;$INPUT lists data items to be input to NONMEM, items have to match the
      data file

$DATA C:\MEROPENEMeva\PKDatafiles\data10.csv IGNORE=@
      ;$DATA specifies name or path of data file. Data file should be comma
      delimited file

$SUBROUTINE ADVAN1 TRANS1
; One-comp model
      ;SOUBROUTINE specifies which model from PREDPP (prediction for population
      pharmacokinetics) is to be used to fit the data

$PK
WTKG = WT/1000
T50  = THETA(3)
HILL = THETA(4)
MF   = PMA**HILL/(PMA**HILL+T50**HILL)
TVCL = THETA(1)*MF*(WTKG/70)**(0.632)   ; typical value of CL
TVV  = THETA(2)*(WTKG/70)               ; typical value of V
;
CL   = TVCL*EXP(ETA(1)) ; individual value of CL
V    = TVV*EXP(ETA(2))  ; individual value of V

S1   = V
K    = CL/V
      ;$PK block assigns thetas to fixed effect parameters (e.g. CL,V)
      ;THETA is the population value, ETA is the between-subject variability
      ;random effects model (e.g. exponential) for structural model parameters
      is specified

$ERROR
 IPRED = A(1)/V
 Y     = IPRED*(1+EPS(1))
      ;$ERROR block specifies a model for residual/within-subject variability
      (e.g. proportional error model)
      ;EPS is the within-subject variability

$THETA (0,10)       ; 1. TVCL (lower bound, initial estimate)
$THETA (0,15)       ; 2. TVV (lower bound, initial estimate)
$THETA (55.4 FIX)   ; 3. T50
$THETA (3.33 FIX)   ; 4. HILL
      ;$THETA specifies initial estimates and bounds for structural model
      parameters

$OMEGA BLOCK(2)
0.1           ; variance for ETA(1), initial estimate
0.01 0.1      ; COvariance ETA(1)-ETA(2), var for ETA(2), initial estimate
      ;$OMEGA specifies initial estimates of the variance of between-subject
      variability and covariance

$SIGMA 0.1   ; variance PROP res error, initial estimate
      ;$SIGMA specifies initial estimates of the variance of residual/within-
      subject variability
```

```
$ESTIMATION METHOD=1 INTER MAXEVAL=9999 PRINT=1  ; calculation method
       ;$ESTIMATION sets condition for estimation of parameters

$COVARIANCE  ; SE of estimate is calculated
       ;$COVARIANCE provides standard errors of estimates

$TABLE ID TIME IPRED CWRES              NOPRINT ONEHEADER FILE=sdtab40
$TABLE ID CL V ETA(1) ETA(2)            NOPRINT NOAPPEND ONEHEADER FILE=patab40
$TABLE ID WT GA PNA PMA                 NOPRINT NOAPPEND ONEHEADER FILE=cotab40
       ;$TABLE specifies generation of tables
```

Table 8.1: A part of the data file used for the development of the population pharmacokinetic model

ID	IDORIG	TIME	AMT	RATE	WT	DV	EVID	SS	II	GA	PNA	PMA	CREA
1	101	0	16	32	846	0	1	1	12	26.43	3.14	29.57	42
1	101	12	0	0	846	2.9	0	0	0	26.43	3.14	29.57	42
1	101	12	16	32	846	0	1	0	0	26.43	3.14	29.57	42
1	101	12.5	0	0	846	149.6	0	0	0	26.43	3.14	29.57	42
1	101	13.5	0	0	846	91.2	0	0	0	26.43	3.14	29.57	42
1	101	16	0	0	846	44.3	0	0	0	26.43	3.14	29.57	42
1	101	20	0	0	846	18.8	0	0	0	26.43	3.14	29.57	42
1	101	24	0	0	846	6.1	0	0	0	26.43	3.14	29.57	42

9. FINAL MODEL FILE FOR INFUSION LENGTH OPTIMIZATION

```
$PROBLEM 1 COMP MERO
;; 1. Based on:                    PK Model for Meropenem
;; 2. Description:                 1-cmt model, IV infusion, optimization
;; 3. Label:                       N/A
;; 4. Structural model:            1-compartment, IV infusion
;; 5. Covariate model:             N/A - using individual PK parameters
;; 6. Inter-individual variability:  0
;; 7. Inter-occasion variability:    0
;; 8. Residual variability:        Additive
;; 9. Estimation:                  FOCE
      ;$PROBLEM specifies the title of the problem

$INPUT ID TIME DV EVID AMT=DROP WT GEST CRET PNAG PMAG SS=DROP II=DROP ICL IV
MIC=DROP RATE=DROP ABC ROW
      ;$INPUT lists data items to be input to NONMEM, items have to match the
      data file

$DATA C:\MEROPENEMeva\PKDatafiles\SimOpt_J.csv IGNORE=@
      ;$DATA specifies name or path of data file. Data file should be comma
      delimited file

$SUBROUTINE ADVAN6 TOL=6
      ;SOUBROUTINE specifies which model from PREDPP (prediction for population
      pharmacokinetics) is to be used to fit the data

$MODEL
 COMP=(TARGET)

$PK
MIC = 2
DOSE  =  20*WT
DUR = THETA(1)*EXP(ETA(1))
CL = ICL
V  = IV
K   =  CL/V
C1=1/V ; coefficient
L=CL/V ; exponent
GAM   =  99   ;to be used for calculation of time above MIC; exponent in Hill eq.
      ;$PK block assigns thetas to fixed effect parameters (e.g. duration)

$DES
IF (T.LE.DUR) THEN
TY = DOSE/DUR*C1/L*(1-EXP(-L*T))
ELSE
TY = DOSE/DUR*C1/L*(1-EXP(-L*DUR))*EXP(-L*(T-DUR))
ENDIF
CONC = TY
DADT(1) = CONC**GAM/(CONC**GAM+MIC**GAM)  ;for calculation of TMIC
      ;$DES specifies differential equations used

$ERROR
TMIC=A(1)
FTAU=(TMIC/12)
IF(ABC.EQ.1) Y=LOG(FTAU)+EPS(1)
      ;$ERROR block specifies a model for residual/within-subject variability
      (e.g. additive error model)
      ;EPS is the within-subject variability

$THETA  (0,1)
      ;$THETA specifies initial estimates and bounds for structural model
```

60

```
        parameters

$OMEGA  0 FIX
      ;$OMEGA specifies initial estimates of the variance of between-subject
      variability

$SIGMA  0.001
      ;$SIGMA specifies initial estimates of the variance of residual/within-
      subject variability

$EST METHOD=COND MAXEVAL=9999 INTERACTION PRINT=1
      ;$ESTIMATION sets condition for estimation of parameters

$COVARIANCE
      ;$COVARIANCE provides standard errors of estimates

$TABLE ID EVID TIME DOSE DV TMIC DUR FTAU TY ICL IV MIC WT ONEHEADER NOPRINT
FILE=sdtabERR25
      ;$TABLE specifies generation of tables
```

Table 9.1: A part of the data file used for the optimization of the infusion length

ID	TIME	DV	EVID	AMT	WT	GEST	CRET	PNAG	PMAG	SS	II	iCL	iV	MIC	RATE	CMT	ROW
1	0	0	2	0	0.93	28.71	40	0.57	29.28	0	0	0.04	0.3	2	0	1	1
1	1	0	2	0	0.93	28.71	40	0.57	29.28	0	0	0.04	0.3	2	0	1	2
1	2	0	2	0	0.93	28.71	40	0.57	29.28	0	0	0.04	0.3	2	0	1	3
1	4	0	2	0	0.93	28.71	40	0.57	29.28	0	0	0.04	0.3	2	0	1	4
1	6	0	2	0	0.93	28.71	40	0.57	29.28	0	0	0.04	0.3	2	0	1	5
1	8	0	2	0	0.93	28.71	40	0.57	29.28	0	0	0.04	0.3	2	0	1	6
1	12	0	0	0	0.93	28.71	40	0.57	29.28	0	0	0.04	0.3	2	0	1	7